Improvement of Brain Source Modeling Based on Multichannel EEG Recordings after Pain Stimulation

Improvement of Brain Source Modeling Based on Multichannel EEG Recordings after Pain Stimulation

PhD Thesis by

Dina Lelic

Mech-Sense, Department of Gastroenterology and Hepatology,
Aalborg Hospital
Arhus University Hospital
Center for Sensory-Motor Interactions (SMI),
Department of Health Science and Technology, Aalborg University

River Publishers
Aalborg

ISBN 978-87-92329-92-9 (e-book)

Published, sold and distributed by:
River Publishers
P.O. Box 1657
Algade 42
9000 Aalborg
Denmark

Tel.: +45369953197
www.riverpublishers.com

The present thesis is partly based on the papers below, which are referred to in the text by Roman numerals. The studies have been carried out in the period from 2007 to 2010 at 1) Mech-Sense, Department of Gastroenterology and Hepatology, Aalborg Hospital, Århus University Hospital & 2) Center for Sensory-Motor Interactions (SMI), Department of Health Science and Technology, Aalborg University.

I: Lelic D, Gratkowski M, Valeriani M, Arendt-Nielsen L, Drewes AM (2009)
Inverse modelling on decomposed electroencephalogram data: a way forward? *Journal of Clinical Neurophysiology.*

II: Lelic D, Gratkowski M, Hennings K, Drewes AM (2010)
Multichannel matching pursuit validation and clustering - a simulation and empirical study. *Journal of Neuroscience Methods.*

III: Lelic D, Olesen AE, Brock C, Staahl C, Drewes AM (2010)
Advanced Pharmaco-EEG Reveals Morphine Induced Changes in the Brain's Pain Network. *Resubmitted to Journal of Clinical Neurophysiology.*

Acknowledgements

This Ph.D. thesis is based on the experimental investigations carried out from 2007 to 2010, during my employment at Mech-Sense, Department of Gastroenterology, Aalborg Hospital, Aarhus University & Centre for Sensory-Motor Interactions (SMI), Department of Health Science and Technology, Aalborg University. The experiments were carried out at the research laboratories at Department of Gastroenterology, Aalborg Hospital and at the GI Physiology Unit, Royal London Hospital.

I owe my most sincere gratitude to my main supervisor Professor M.D., Ph.D., DMSc., Asbjørn Mohr Drewes, for outstanding inspiration, encouragement, supervision and constructive criticism of my work and manuscripts. I also want to thank the head of department, M.D., DMSc. Ulrik Tage-Jensen, Department of Medical Gastroenterology and M.D., DMSc., MPM Hans Gregersen, former Director of Mech-Sense for providing excellent working conditions for research.

I want to express my gratitude to M.Sc., Ph.D. Maciej Gratowski from Technische Universität Ilmenau, Ilmenau, Germany for the fruitful discussions regarding the technical work and data analysis during my PhD.

I want to further express my gratitude to M.D., Ph.D. Massimiliano Valeriani, from Division of Neurology, Ospedale Pediatrico Bambino Gesù, IRCCS, Rome, Italy, for great discussions and his neurophysiological insight during my first study.

It is important for me to thank my former colleague M.Sc., Ph.D. Kristian Hennings. He was briefly involved in my PhD, but has influenced it positively nonetheless, by being involved in the early developments of the clustering algorithm and offering great discussions of new ideas.

I want to thank my colleagues DVM, Ph.D. Christina Brock, M.Sc.Pharm, Ph.D. Anne Estrup Olesen, M.Sc.Pharm, Ph.D. Camilla Staahl, M.D. Søren Schou Olesen, M.D., Ph.D. Anne Krarup, and M.Sc.Pharm. Trine Andresen for rewarding discussions in the office and for contributing much to my medical/pharmaceutical knowledge. For practical assistance during experiments, I have to thank the outstanding Mech-Sense research nurses Isabelle M. Larsen and Birgit Koch-Henriksen. I am further indebted to Isabelle M. Larsen for always being so fast to respond to my enquiries regarding the rectal studies in London and to send little things we were missing during my stay there. I have to thank M.Sc., Ph.D. Flemming Graversen for his technical help. I want to thank all of my colleagues, also including lab technician Anne Brokjær, M.D., Ph.D. Jens Brøndum Frøkjær, M.Sc. Tine Maria Hansen, and M.Sc. Carina Graversen, for creating a positive working environment and making my stay at Mech-Sense very pleasant. Britta Lund and Susanne Nielsen Lundis are thanked for secretarial help.

I thank my collaborators M.B.B.S. Rebecca Burgell and M.D. Emma Carrington at the Royal London Hospital for the successful recruitment of patients, for creating wonderful working environment in the lab, and in general, making my stay in London very pleasant.

I express my gratitude to all the volunteers who participated in the experiments, without whom, none of the studies would have been possible

This PhD was funded by Danish Agency for Science, Technology, and Innovation and Karen Elise Jensen Foundation.

Last but not least, I want to thank my family, especially my parents, Muhidin & Verica, and my sister Merima, for their never-ending support during my scientific work. They deserve the dedication of this thesis.

Dina Lelic; October 14nd 2010, Aalborg, Denmark.

List of Abbreviations

ACC: Anterior cingulated cortex

BAEP: Brainstem auditory evoked potentials

BESA: Brain electric source analysis

BSS: Blind source separation

CP: constipated patient

EEG: Electroencephalogram

EP: Evoked potentials

fMRI: Functional magnetic resonance imaging

HV: healthy volunteer

ICA: Independent component analysis

LORETA: Low-resolution electromagnetic tomography

MEG: Magnetoencephalography

MMP: Multichannel matching pursuit

MP: Matching pursuit

MUSIC: Multiple signal classification

PM: Pre-motor

PET: Positron emission tomography

R-MUSIC: Recursive multiple signal classification

RAP- MUSIC: Recursively applied and projected multiple signal classification

RH: Rectal hyposensitivity

SEP: Somatosensory evoked potentials

SI: Primary somatosensory cortex

SII: Secondary somatosensory cortex

SNR: Signal to noise ratio

SOBI: Second order blind identification

Thal: Thalamus

VAS: Visual analogue scale

1. Introduction

Chronic pain of moderate to severe intensity occurs in 19% of adult Europeans, seriously affecting the quality of their social and working lives. Very few are managed by pain specialists and nearly half receive inadequate pain management(Breivik, Collett et al., 2006). In order to understand and better treat these patients, understanding of pain processing in the brain is necessary. Until today, this knowledge is very limited and therefore further research in and focus on brain processing of pain is warranted.

1.1 Experimental pain

Studies of clinical pain are limited by bias due to cognitive, emotional, and social aspects of the disease. Therefore, pain is a multi-dimensional, highly individual perception, difficult to quantify and validate in clinical settings. The great individual differences and affiliated symptoms that especially follow visceral pain make it difficult to study basic pain manifestations or the effect of pharmacological treatment. Thus, the effect on e.g., nausea and anxiety may be difficult to distinguish from pain relief in the clinical settings. When applying experimental pain in healthy volunteers some of these bias are overcome and the quality and intensity of painful stimuli can be reported reproducibly(Staahl, Reddy et al., 2006). Therefore, experimental human pain models appear to be better suited to study pain mechanisms.

In standardized experimental pain studies, it is possible to control precisely the localization, intensity, duration, and modality of the stimulus(Drewes, Gregersen et al., 2003). The evoked sensations can be assessed with subjective methods quantitatively by using a visual analogue scale (VAS) and qualitatively (e.g. by using the McGill Pain Questionnaire), and stimulus-response relationships can be investigated. Objective, physiological responses to pain can be recorded with e.g., cerebral evoked potentials (EP).

1.2 Imaging of pain in the brain

Several studies have indicated a set of cortical and sub-cortical areas processing nociceptive information. These areas have in turn been referred to as the pain matrix(Brooks and Tracey, 2005;Iannetti and Mouraux, 2010). Until today, the modalities used to clinically image pain activity in the brain have typically been functional magnetic resonance imaging (fMRI) and positron emission tomography (PET). These modalities have the advantage of excellent spatial resolution, meaning that by looking at fMRI or PET scan, it is possible to say exactly where activity in the brain is occurring. However, the disadvantage is the temporal resolution on scale of seconds and minutes. Due to this, it is impossible to monitor sequential activation of the sources. Instead, the scan shows an overall picture of all the sources that are active, including non-pain specific sources such as cognitive and emotional responses. In contrast to fMRI and PET, EPs have excellent temporal resolution on millisecond scale. With its time-resolution on millisecond scale this approach allows distinction between exogenous (pain specific) processing that approximately takes place within the first 200 ms, and later endogenous (unspecific) brain

activation(Hobson, Furlong et al., 2005). However, the spatial resolution is poor and it is impossible to tell where in the brain these potentials are coming from. Several algorithms have been proposed and implemented in order to model the location and strength of active brain sources underlying the EP signal. This is known as “inverse modeling”.

1.3 Inverse modeling of evoked potentials

The process of predicting the locations of the sources of EPs measured on the scalp is termed inverse modeling. Inverse modeling is an ill-posed and underdetermined problem(Koles, 1998). Given a restricted number of electrodes on the scalp, an infinite number of brain source configurations could account for the same signal distribution recorded on the scalp. Theoretically speaking, only an infinite number of electrodes on the scalp would enable for a unique solution of the source location responsible for signal generation on the scalp. However, by placing certain constraints on the possible solution, i.e. number of sources and physiologically plausible locations, the inverse problem can be solved. Inverse modeling algorithms have been usually applied to instantaneous EP data with 4 main disadvantages: 1) the need to start from a pre-determined hypothesis, at least concerning the number of sources and the brain area where they are active, 2) the instability of algorithms to effectively model multiple sources, 3) the interference of background noise, and 4) the difficulty to adequately model deep sources. Factors such as head modeling errors, physiological noise (blinks, muscle artifacts, etc) and electrical noise affect the solution(Whittingstall, Stroink et al., 2003). Although a conceivable hypothesis about the source number can be made on the base of the physiological and anatomical knowledge, it would be much better to have a tool disentangling the different dominating sources present prior to investigation. For this reason, several signal decomposition algorithms have been proposed and validated.

1.4 Signal decomposition of evoked potentials

Space-time based signal decompositions have typically been used prior to inverse modeling, such as Blind Source Separation (BSS). However, these algorithms place some strong assumptions on the data among which are linearity and some statistical independence of the sources(Durka, Matysiak et al., 2005). Furthermore, BSS algorithms assume that there are less than or equal number of sources as there are sensors and they try to estimate the number of sources by data reduction techniques(Durka, Matysiak et al., 2005). This leads to a risk of overestimating the number of sources with data over-fitting. In contrast to BSS methods, there is a relatively new signal decomposition method, Multichannel Matching Pursuit (MMP) where the electroencephalogram (EEG) data is decomposed into a sum of waveforms (usually termed atoms) chosen from an over-complete dictionary of atoms, each being defined in time, frequency, and space(Durka, Matysiak et al., 2005). MMP is an iterative algorithm where the first iteration finds the atom that optimally fits the data, and in subsequent iterations, it finds the atoms which optimally fit the residual left after the previous result has been subtracted from the data. The user can choose the residuum

threshold or the number of iterations to indicate when the algorithm should stop iterating. This overcomes the limitation of calculating the number of components in the data and also MMP avoids the strong assumptions made by BSS algorithms. Nevertheless, thus far MMP has not been sufficiently validated by studies of source localization on either simulated or empirical EEG data.

1.5 Automation of multichannel matching pursuit and inverse modeling

Typically, MMP followed by source localization is applied to a single subject at a time. As there can be many atoms per subject, this approach makes it difficult to study group differences, i.e. group of patients versus group of healthy controls. One of the methods to study common sources within a group is grand mean analysis. However, the major shortcoming of this approach is that small differences in brain activation between a few subjects can contaminate the entire solution. Furthermore, more qualitative information such as time and frequency of the waveforms of the sources is not taken into consideration. Another approach is to classify all the differences/similarities between subjects in different groups visually. This process can be tedious and lead to subjective bias, especially when dealing with datasets of many subjects. It would be much better to have a tool to automatically process all the data and output the common features within a group. This method would make it easier to observe any differences or similarities between groups.

1.6 Aims of this thesis

The overall objectives of this project were to improve the existing source localization methods, to automate EP signal analysis, and make them more applicable to pain and drug studies. Therefore, the aims of this thesis were:

1. For both simulated and empirical data, to compare accuracy between inverse modeling done on a) instantaneous EPs peak by peak, b) commonly used signal decomposition methods (independent component analysis (ICA) and second-order blind identification (SOBI)), and c) MMP.
2. To test the limitations of MMP as the level of noise and number of sources increase.
3. To develop a clustering method for MMP atoms such that analysis can be automated and overview is not lost.
4. To validate the clustering method on simulated and empirical EP data.
5. To apply MMP and clustering method to visceral pain data in order to study how the brain activity due to pain is altered after morphine administration.
6. To investigate whether there are signs of cortical reorganization on preliminary rectal evoked potential data in constipated patients with rectal hyposensitivity.

2. The pain system

According to The World Health Organization, pain is defined as “an unpleasant sensory or emotional experience associated with actual or potential tissue damage, or described in terms of such damage.” From this perspective, pain can be seen as awareness which signals the body that if nothing is done, the body is at risk of getting hurt.

Nociceptive pain occurs when the nociceptors are stimulated by chemical, thermal, or mechanical stimulation. Nociceptors are nerve endings that react to potentially damaging stimuli by sending signals to the spinal cord and brain and are located in skin, internal organs, joints, muscles and tendons. There are two types of nociceptors and these are Aδ-myelinated and C-polymodal. Aδ nociceptors respond to mechanical stimulation, especially pinching or pinpricks, and conduct at 5-30 m/s. They are responsible for conducting the “first pain” occurring immediately after the noxious stimulus. In the skin Aδ-fibres are mainly specialized for detection of dangerous mechanical and thermal stresses and for triggering a rapid nociceptive response and protective reflexes(Byers and Bonica, 2001). Some Aδ nociceptors also respond to heat stimuli. C-fibers constitute the greatest number of nociceptors in peripheral nerves. Their conduction velocity is less than 1 m/s. The C nociceptors respond to mechanical, thermal or chemical stimuli applied to the skin. C-fibres are responsible for conducting the “second pain” which is the dull, burning sensation felt after the “first pain”. There are two kinds of nociceptive pain: somatic and visceral. Somatic pain occurs when skin, muscle, or bone is damaged, whereas visceral pain occurs in the internal organs. Somatic pain is often regarded as a sharp pain localized in a specific area of injury. Visceral pain, on the other hand, comes from organs which are not heavily supplied by nociceptors, and therefore the pain may feel dull and vague and harder to pinpoint. Another peculiarity about visceral pain is the fact that it is often felt in places distant from the location of the affected organ, i.e. pain in the left arm due to heart attack.

Neuropathic pain is another entity. According to Treede et al., neuropathic pain is defined as “pain arising as a direct consequence of a lesion or disease affecting the somatosensory system(Treede, Jensen et al., 2008).” However, in a large number of patients it may still be impossible to distinguish between inflammatory and neuropathic pain and therefore a proper definition of neuropathic pain has not yet been reached. Neuropathic pain is typically chronic as it may persist for months or years after injury and unlike nociceptive pain, it does not require a stimulation of specific pain receptors(Pazzaglia and Valeriani, 2009). Neuropathic pain can occur when nerves that usually respond to an injury become active for no reason. With neuropathic pain, the function of the nerves becomes compromised and nerve activity increases. This activity causes other nerves to become ultra-sensitive, leading to altered responses to felt sensations, such as allodynia or hyperalgesia. Allodynia refers to stimuli that are not normally painful becoming painful and hyperalgesia refers to painful stimuli being experienced as more painful than usual(Guyton and Hall, 2006;Gould, 2007;Hanline, 2007).

2.1 Processing of pain in the brain

Although involvement of the cerebral cortex in pain processing has been doubted for many decades, in recent years an extensive cortical network associated with pain processing has been exposed and is increasingly recognized as playing a major role in the representation and modulation of pain. There is a growing consensus regarding the crucial cortical areas and the connectivity between them from human and animal experimental studies (see figure 1). These areas are termed the pain matrix(Iannetti and Mouraux, 2010) and most often include: primary somatosensory cortex (SI), secondary somatosensory cortex (SII), the anterior cingulate cortex (ACC), and the insular cortex. The involvement of each area's pain processing is described in the following subsections.

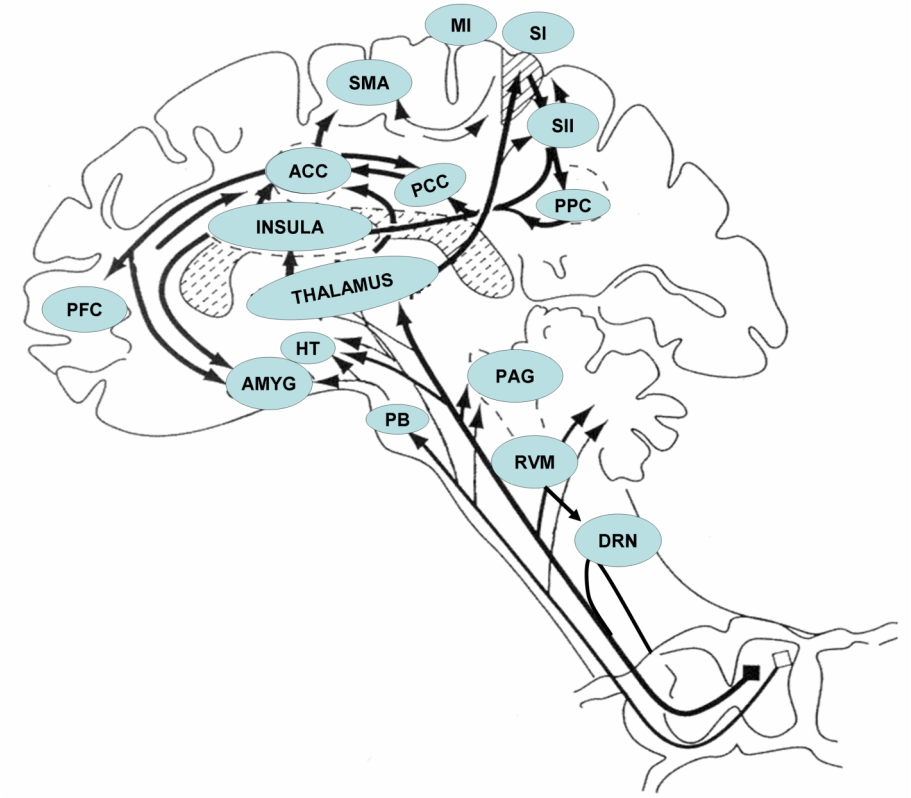

Figure 1.A drawing of the subcortical and cortical structures, which are activated in response to pain. Abbreviations: DRN: dorsal reticular nucleus; RVM: rostroventral medulla; PAG: periaqueductal grey; PB: parabrachial nucleus of the dorsolateral pons; AMYG: amygdale; HT: hypothalamus; ACC: anterior cingulate cortex; PCC: posterior cingulate cortex; PPC: posterior parietal complex; SI + SII: primary and secondary somatosensory cortices respectively; MI: motor cortex; SMA: supplementary motor area and PFC: prefrontal cortex; Adapted and modified from(Price, 2000).

2.1.1 Primary somatosensory cortex

Although, the role of SI in pain processing is controversial and has long been disputed, recent anatomical, neurophysiological, and imaging data confirm the role of SI in pain processing. Overall, these findings point to a specific role of SI in sensory-discriminative functions of pain perception, such as spatial

discrimination and intensity coding. Electrophysiologically, single cell recordings in rats, and anesthetized and awake monkeys showed neurons in SI that responded to noxious stimuli(Lamour, Willer et al., 1983;Kenshalo and Isensee, 1983;Kenshalo, Chudler et al., 1988;Chudler, Anton et al., 1990). Most of these nociceptive SI neurons were arranged somatotopically and had limited receptive fields. The activity of these neurons correlated with duration, intensity of the stimulus, and intensity of stimulus perception. PET, fMRI, and MEG/EEG studies in humans have provided evidence for contribution of SI in pain processing(Tarkka and Treede, 1993;Casey, Minoshima et al., 1994;Andersson, Lilja et al., 1997;Derbyshire, Jones et al., 1997;Iadarola, Berman et al., 1998;Ploner, Schmitz et al., 1999). A number of studies have reported the somatotopic arrangement of pain in SI to be along the central sulcus which strongly suggests that this region is involved in localization of painful stimuli on the body surface(Tarkka and Treede, 1993;Schnitzler and Ploner, 2000). Furthermore, a case report demonstrated that localization of painful stimuli may be greatly impaired when SI is damaged(Ploner, Freund et al., 1999). Other imaging data showed that activity of SI correlates with the level of pain sensation but not with the level of pain unpleasantness. However, regardless of the plausible role of SI in pain processing, a significant amount of data suggests SI may also serve to modulate tactile perception(Ploner, Schmitz et al., 1999;Bushnell, Duncan et al., 1999). Therefore, SI may be involved in perception and modulation of both painful and nonpainful somatosensory stimuli.

2.1.2 Secondary somatosensory cortex

Neurophysiologic and functional imaging data indicate participation of SII in human pain processing. Anatomic studies indicate that SII receives nociceptive projections from lateral thalamic nuclei which originate predominantly from the ventral posterior inferior thalamic nucleus(Stevens, London et al., 1993). Contrary to most SI cells, nociceptive neurons in SII have mostly large, bilateral receptive fields(Dong, Salonen et al., 1989;Dong, Chudler et al., 1994) and hence SII is activated bilaterally during painful stimulation in the periphery. A number of PET, fMRI, MEG, and EEG pain studies have demonstrated involvement of SII(Hari, Kaukoranta et al., 1983;Huttunen, Kobal et al., 1986;Talbot, Marrett et al., 1991;Tarkka and Treede, 1993;Coghill, Talbot et al., 1994;Casey, Minoshima et al., 1994;Kakigi, Koyama et al., 1995;Bromm and Chen, 1995;Spiegel, Hansen et al., 1996;Hari, Portin et al., 1997;Derbyshire, Jones et al., 1997;Davis, Kwan et al., 1998;Iadarola, Berman et al., 1998;Coghill, Sang et al., 1999;Ploner, Schmitz et al., 1999;Ploner, Schmitz et al., 2000;Torquati, Pizzella et al., 2002;Brooks, Nurmikko et al., 2002;Fitzek, Fitzek et al., 2004;Ferretti, Del Gratta et al., 2004;Drewes, Dimcevski et al., 2006). Generally, activations are observed bilaterally in the upper bank of the Sylvian fissure(Schnitzler and Ploner, 2000;Valeriani, Le Pera et al., 2001). Temporally, MEG recordings showed nearly simultaneous activity of SI and SII to selective nociceptive stimuli indicating parallel activation of these areas(Ploner, Schmitz et al., 1999). In contrast to this, it has been shown that after painless tactile stimuli, there was sequential activity of SI followed by SII(Hari, Karhu et al., 1993;Schnitzler, Volkmann

et al., 1999;Ploner, Schmitz et al., 2000). These temporal activation patterns suggest essentially different processing in humans for tactile and nociceptive information(Schnitzler and Ploner, 2000). Furthermore, the temporal activation pattern of SI and SII strongly supports direct thalamocortical distribution of nociceptive information to SII(Schnitzler and Ploner, 2000). SII projects via the insula to the temporal lobe limbic structures(Shi and Cassell, 1998a). These corticolimbic projections have been proposed to subserve tactile learning and memory such as roughness discrimination and object size detection(Schnitzler and Ploner, 2000).

2.1.3 Insula

Numerous functional imaging studies indicate participation of insula in human pain processing and it is the most frequently activated structure in fMRI studies of pain(Apkarian, Bushnell et al., 2005). Insula appears to receive information via a direct thalamo-insular connection and can be thought of as a site for sensory and affective integration. Thalamo-cortical connectivity as well as results from physiologic studies imply that the posterior parts of the insula are mainly involved in auditory, visual, and somatosensory functions, whereas the anterior parts of the insula are predominantly involved in olfactory, gustatory, and viscero-autonomic functions(Augustine, 1996). In addition, the insula receives afferents from SII and projects to the amygdala and hippocampal formation, and has thus been proposed to subserve tactile and pain related learning and memory(Lenz, Gracely et al., 1997;Shi and Cassell, 1998a;Shi and Cassell, 1998b). The insula may integrate pain-related input from SII and the thalamus with contextual information from other modalities before relaying this information to the temporal lobe limbic structures(Schnitzler and Ploner, 2000). In visceral EP studies, the insula has also been shown to be involved in pain processing(Drewes, Dimcevski et al., 2006;Dimcevski, Sami et al., 2007).

2.1.4 Anterior cingulate cortex / pre-frontal cortex

The ACC mainly receives extensive projections from the mediodorsal thalamic nucleus and broadly connects with relevant regions of the descending modulation system, including PAG and amygdala(Ploner and Schnitzler, 2004;Wang and Shyu, 2004;Xie, Huo et al., 2009). Both visceral and cutenous specific nociceptive neurons have frequently been found in the ACC of rabbit, suggesting that the ACC is associated with both visceral and somatic pain(Sikes, Vogt et al., 2008). Further studies revealed that ACC nociceptive neurons are involved in attention to pain and escape from pain but not in sensation of pain(Iwata, Kamo et al., 2005). Most of brain imaging studies in humans have reported activation of ACC(Rainville, Duncan et al., 1997;Laurent, Peyron et al., 2000;Mohr, Binkofski et al., 2005). Several studies suggest that the ACC is involved in encoding the level of certainty of expected painful stimuli(Mohr, Binkofski et al., 2005). Expectation of reduced pain perception due to placebo medication is associated with an altered activity in the anterior ACC(Petrovic, Kalso et al., 2002;Wager, Rilling et al., 2004). ACC should not be considered a mere pain center as it is activated by other various

cognitive and attentional tasks(Petersen, Fox et al., 1988;Corbetta, Miezin et al., 1991;Devinsky, Morrell et al., 1995). Consequently, pain-related activations may correspond to a non-pain specific effect. Although, direct comparison of pain and attention related activations showed that they do not spatially correspond to each other(Davis, Taylor et al., 1997;Derbyshire, Vogt et al., 1998); meaning that pain-related activations of ACC are not solely due to attention effects. This, in addition to the proximity of nociceptive, motor, and cognitive regions of the ACC suggests possible local interconnections that may allow the output of the ACC pain area to command immediate behavioral reactions(Schnitzler and Ploner, 2000).

Activation of the prefrontal cortex has also been observed in response to both somatic and visceral sensation. It interacts with the ACC and is believed to be responsible for cognitive evaluation, self-awareness, attention, and behavioral control(Bingel and Tracey, 2008). Pre-frontal cortex has been suggested as an important region in placebo analgesia(Petrovic, Kalso et al., 2002;Bingel and Tracey, 2008;Krummenacher, Candia et al., 2010). The rostral ACC/prefrontal cortex also contain a high concentration of opioid receptors and have been suggested as an important region in opioid analgesia(Petrovic, Kalso et al., 2002). In III, we found that centre of activity of brain sources due to electrical pain stimulation of esophagus shifts toward the rostral ACC/pre-frontal cortex after morphine administration.

3. Electroencephalogram and evoked potentials

An EP is an electrical potential recorded from the nervous system following a presentation of a stimulus, such as pain on surface or viscera. EP amplitudes tend to be low as compared to amplitudes of spontaneous EEG activity. In order to decode the evoked potentials from the background EEG activity and noise, signal averaging is necessary. Provided enough of recorded trials, the evoked potentials become bigger in amplitude and therefore visible and the random background activity cancels out (see figure 2). Then, the EP latencies and amplitudes of the peaks can be analyzed by visual inspection. Recently, a number of methods have been proposed in order to automate EP peak detection. We have also presented such a method for segmenting EPs into functional micro-states(Hennings, Lelic et al., 2009).

The main advantage of using EPs to study processing of pain in the brain is its excellent time resolution (millisecond scale). Since exogenous response to pain takes place within the first ~=200ms following the stimulus, EPs are an excellent tool to monitor sequential brain activity due to pain. A disadvantage of EPs is the poor spatial resolution. The signal travels from the brain source to the scalp via volume conduction through several tissues above the brain and therefore by the time it arrives to the scalp it is distorted. On the contrary to EPs, fMRI and PET have excellent spatial resolution and until today they are the main imaging modalities used to understand brain's processing of pain. However, fMRI and PET have insufficient time resolution (on scales of seconds and minutes). Therefore, a lot of brain activity seen with these imaging methods is not pain specific and it is difficult to separate the pain specific activity from non-specific, i.e. emotional and cognitive responses. We have published a review about different imaging methods discussed in this thesis (i.e. fMRI, PET, EPs) and their advantages and limitations(Sharma, Lelic et al., 2009). We have also discussed the advantages of EP over imaging modalities such as fMRI and PET in a review regarding modeling of brain activity to gastrointestinal pain(Liao, Lelic et al., 2008). Ideally, a combination of EP's time resolution and fMRI and PET spatial resolution should be achieved (see figure 3). This can be done by detecting which brain sources are generating the EPs recorded on the scalp. This is known as the EEG inverse problem which is discussed in chapter 4.

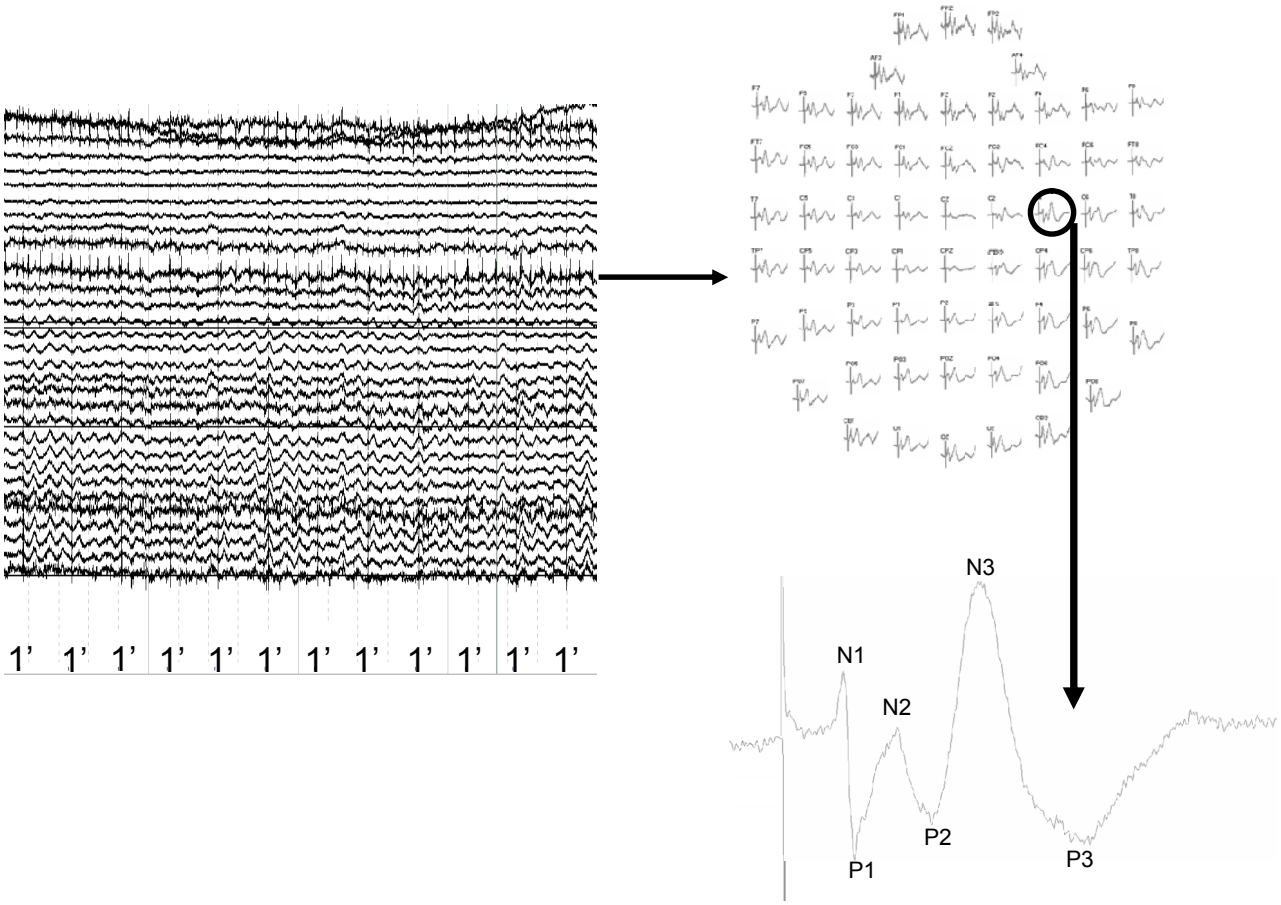

Figure 2. An example of an evoked potential signal. To the left of the figure: raw EEG traces. Each 1’ represents the time point when the stimulus was presented. This data can be epoched at each stimulus point for a certain number of milliseconds (i.e. 150ms) and then these epochs can be averaged in order to obtain the averaged data (EPs) presented at the upper right of the figure. The figure represents averages from 62 scalp electrodes. Data from one of the electrodes was zoomed in and presented at the bottom right of the figure for illustration. Now it is possible to see brain responses due to stimulus as peaks in time. The spike-like peak before N1 is the stimulus artifact and the trace before is baseline EEG before presentation of the stimulus.

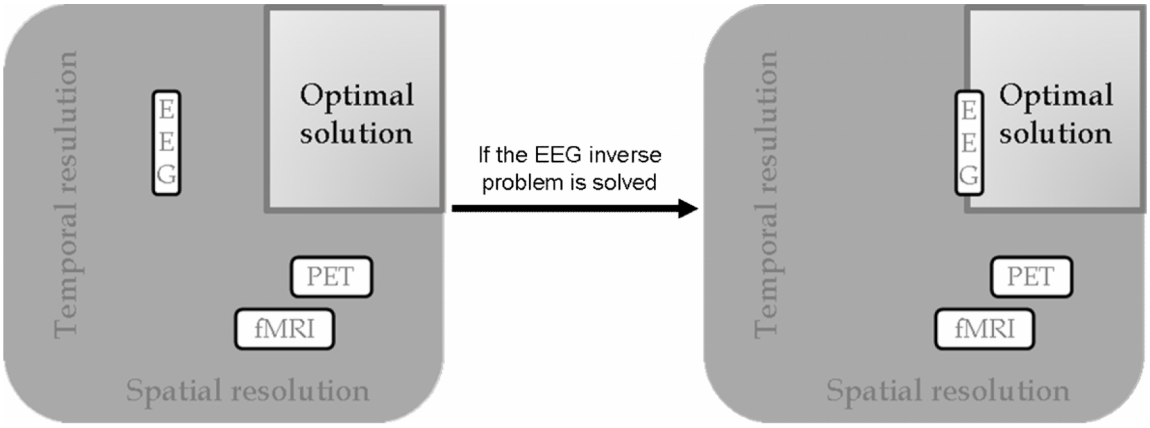

Figure 3. Illustration of relative temporal and spatial resolution of EEG, fMRI and PET. Left: Current resolution properties; it is seen that the temporal resolution of EEG is high while spatial resolution is low. Contrary, spatial resolution of PET and fMRI is high, whereas temporal resolution is low. Right: If the EEG inverse problem is solved, high spatial resolution can be achieved with EEG while the temporal resolution is also kept high.

3.1 Generators of evoked potentials

Differences of electrical potentials recorded on the scalp are caused by summed postsynaptic graded potentials from pyramidal cells that create current dipoles between the soma (body of the neuron) and apical dendrites, which branch from neurons(Sanei and Chambers, 2007). Approximately, 85% of all cortical neurons are these pyramidal cells. Apart from having more or less synchronous activity, the neurons need be regularly arranged to have a measurable scalp EEG signal. The spatial properties of the neurons must be so that they amplify each other's extracellular potential fields. The neighboring pyramidal cells are organized so that the axes of their dendrite tree are parallel with each other and normal to the cortical surface. The factors that influence the size, shape, and duration of EEG signals are: 1) the distance of the recording electrode from the current generator, 2) the duration of the postsynaptic potentials, 3) the number of synchronously activated postsynaptic potentials, and 4) the anatomical orientation of the layer of pyramidal cells generating the current(Schaul, 1998).

The human head consists of different layers including the scalp, skull, and brain. The skull attenuates the signals approximately a hundred times more than the soft tissue. However, most of the noise is generated either within the brain or over the scalp and therefore only large populations of active neurons can generate enough potential to be recordable on the scalp(Sanei and Chambers, 2007). These groups of synchronously active neurons can be mathematically modeled by current dipoles. A dipole is an element with two opposing poles (i.e. a battery). Positive current is absorbed at one end of the pole (the sink) and emanates from the other end (the source), thus leaving the brain electrically neutral (figure 4).

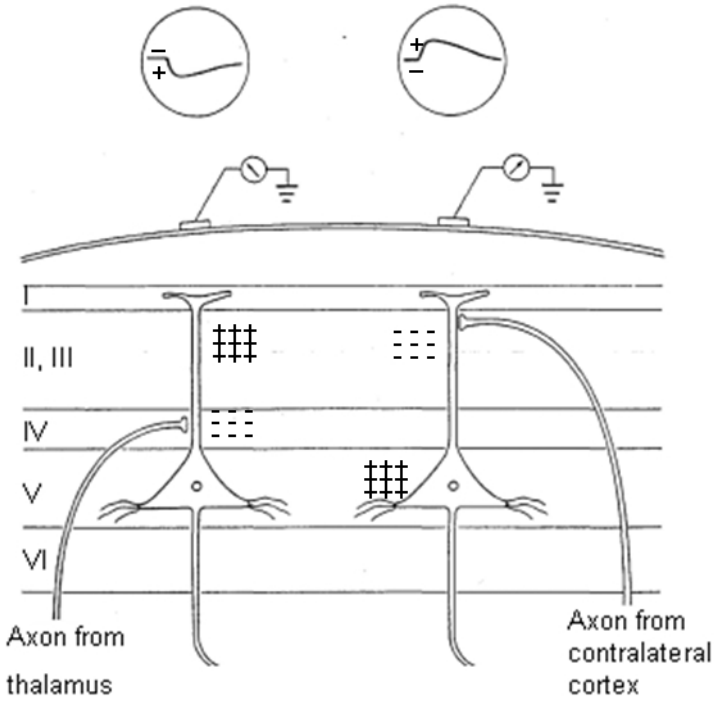

Figure 4. Generation of extracellular voltage fields from graded synaptic activity (adapted from (Martin, 1991)). Each synapse acts like a battery driving current in a small loop and having high internal impedance, so its current strength does not vary with external load. At the top left, the trace shows a negative wave that corresponds to a current sink and at the top right, the trace shows a positive wave that corresponds to a current charge. EEG fields are primarily generated by the large, vertically oriented pyramidal neurons located in cortical layers III, V, and VI.

The electrical field generated from convoluted layers of pyramidal neurons is referred to as an open field. The field potential around an open field decays inversely to the distance from the generator and can be viewed from almost any distance in a volume conductor. There are structures in the central nervous system which are not aligned as dipoles and are referred to as closed fields. There is a lot of debate in the research community regarding structures in thalamus generating closed field potentials and not being large enough to be detected on the scalp(Schaul, 1998). However, a number of studies have showed reproducible results regarding EPs generated by the deep structures, i.e. the thalamus source of P14 in SEPs(Buchner and Scherg, 1991;Buchner, Fuchs et al., 1994), and we showed a brain stem source of EPs around 7-8 ms in BAEPs (II).

3.2 *Frequency bands in the EEG*

The EEG signal can be divided into 5 frequency bands: Delta (up to 4Hz), Theta (4-8 Hz), Alpha (8-12 Hz), Beta (12-30 Hz), and Gamma (above 30 Hz). Each of these frequency bands is associated with a certain brain function, as described below(Sanei and Chambers, 2007):

- Delta: Normally associated with deep sleep and may be present in the waking state; high amplitude waves.
- Theta: The waves occur as consciousness slips into drowsiness; a theta wave is often accompanied by other frequencies and seems to be related to the level of arousal; larger contingents of theta wave activity in the waking adult are abnormal and are caused by various pathological conditions.
- Alpha: Normally associated with relaxed state, closing the eyes; found in posterior regions of head and usually appears over occipital regions of the brain, both sides, higher in amplitude on dominant side, central sites at rest.
- Beta: Associated with alert state, active, busy, or anxious thinking, active concentration; found in both sides, symmetrical distribution, most evident frontally; low amplitude waves.
- Gamma: Low in amplitude and their occurrence is rare. Associated with cross-modal sensory processing (i.e. perception that combines two different senses, for example sound and vision); also shown during short term memory matching of recognized objects, sounds, or tactile sensations.
- Higher than normal EEG (200-300 Hz): Have been found in cerebral structures of animals, but they have not played any role in clinical neurophysiology.

3.3 Noise in EEG measurements

Biological or electrical noise can contribute to EEG signals. As far as EPs are concerned, the true signal is only that part of EEG which is generated as a response to the given stimulus, all other brain generated activity is considered as noise. Biological noise can also come from eye movement and blinking. These eye artifacts have considerably higher amplitude than the EEG activity and can be seen in the frontal electrodes. Electrical activity from heart and muscle can also generate artifacts in EEG recordings. Activity from the muscles produce the most severe bioelectric noise because of its frequency spectrum and unlike the activity from the eye and heart, it is impossible to measure activity from the muscle independently from the EEG to be used for noise cancellation. Another main noise contributor to the EEG is the 50Hz noise generated by the power lines. In II, we have shown that brain source localization in combination with MMP is robust due to noise.

4. Inverse modeling of evoked potentials

During the last few decades, the researchers in neuroscience community have been very active in trying to find the underlying sources which generate the EEG. This process consists of solving the inverse and forward problems. The forward problem starts from electrical source configuration representing active neurons in the head. Then the potentials at the scalp electrodes are calculated for this configuration. If the configuration and distribution of sources inside the brain are known at every time instant and the conductive properties of the tissues are known everywhere within the volume of the head, the forward problem is straightforward to solve. The inverse problem tries to do the opposite and find the generating EEG sources from the EEG signal at the scalp electrodes alone (figure 5). On the contrary to the forward problem, the inverse problem is not straight forward to solve. The inverse problem, by definition, has no unique solution. Different source configurations can result in the same distribution of electromagnetic field on the scalp surface. As mentioned earlier, only an infinite number of scalp electrodes would enable a unique determination of the locations of the generating sources. However, if physiologically and physically valid á priori constraints are made and if it is recognized that only one source configuration can be correct, the generating sources can be estimated. The constraints can consist of the number, type, and location of the sources(Malmivuo and Plonsey, 1995;Lagerlund and Worrell, 2005). For example, sources cannot be located in the skull or in the ventricles of the brain(Koles, 1998). This constraint alone will eliminate many of the source configurations that can account for the measurements. The selection of constraints to be placed on the inverse solution is a critical step because an incorrect assortment of these constraints may give a solution which does not provide any physiologically meaningful information about the generators(Michel, Murray et al., 2004;Lagerlund and Worrell, 2005).

There are several approaches to solving the inverse problem and some of the most commonly used methods are summarized in table 1. The inverse models are classified into *overdetermined (dipolar)* models and *underdetermined (current density)* source models.

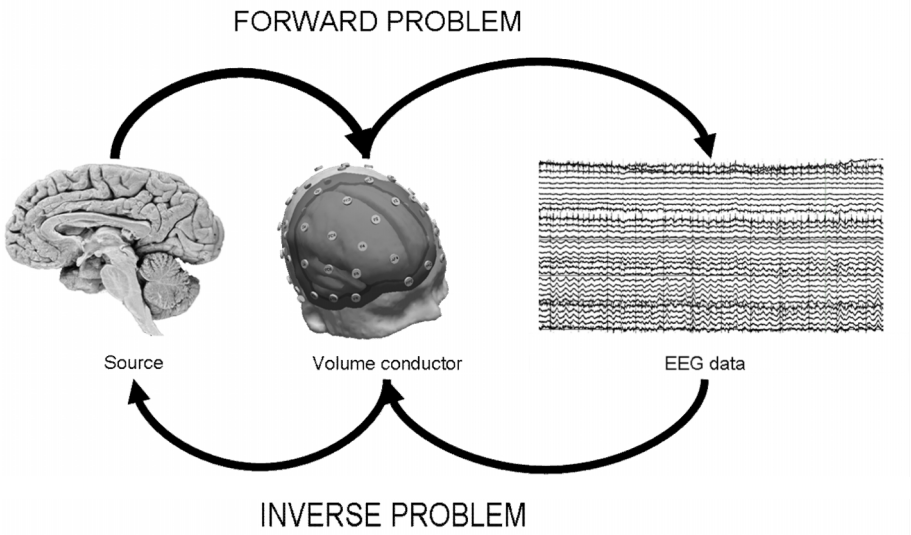

Figure 5. Definition of the forward and the inverse problem. The forward problem constitutes of the signal going from the source, via volume conduction to the scalp where the EEG is recorded. The little circles on top of the head in the center of the figure represent the recording electrodes. The inverse problem constitutes of finding the generating source given the EEG signal alone.

Dipolar models: The basic á priori assumption underlining the dipolar models is that a small number of brain sources can sufficiently describe the signal recorded on the scalp. The best location of these sources is found by computing the surface electric map generated by these sources using a certain forward model and comparing it with the actual signal recorded at the scalp (figure 6). This comparison is usually made by calculating the squared error between two maps and the idea is to minimize this error. A general risk of these methods is that they can get trapped in an undesirable local minima, resulting in the algorithm accepting a certain location because moving in any direction increases the error of the fit(Michel, Murray et al., 2004). Another shortcoming of these types of algorithms is, the more sources there are, the more unstable the algorithm becomes. Mosher et al. stated that decoupling estimation of linear and non-linear parameters of the sources can reduce the complexity and help in identifying the global minimum in multiple source modeling(Mosher, Lewis et al., 1992). However, it is wrong to say that the mathematically global minimum is the correct solution. Among all possible inverse solutions of the data, the global minimum is only slightly more likely to be the best solution. Therefore, it is critical to combine the neurophysiological knowledge with the mathematically provided inverse solution. In order to assist with this, Sherg et al. proposed a spatiotemporal multiple source analysis technique (implemented in the commercial software BESA)(Scherg, Bast et al., 1999). We used this method in a chronic pancreatitis study in order to investigate cerebral pain processing in patients suffering from pain due to chronic pancreatitis (see figure 7)(Olesen, Frøkjær et al., 2010). This method fixes the dipole locations over a given time interval and then uses the whole block of data in the least squares fit. The fitting then results in time varying amplitudes of these sources. The critical issue in this method is to assume the correct number of sources. Two proposed approaches by Sherg and colleagues are: analyze the entire period at

once by increasing the number of sources until the signal unexplained by the sources is minimal or analyze the time period sequentially by adding new dipoles for each time period until the signal unexplained by the sources is minimized. Solutions of this method are very much based on the user's physiological knowledge and assumptions. Several studies have proposed to estimate the number of generating sources based on studies using other imaging methods such as fMRI and PET(Michel, Murray et al., 2004). However, this approach may not be the most favorable as mismatch between the fMRI/PET and EEG measures can be expected for several reasons; for example, fMRI/PET can see the 'close field' areas which EEG is blind to, and EEG is sensitive to short-lasting neuronal activity whereas this activity may not be modeled by fMRI because they don't reach the significance level due to thresholding of fMRI. An alternative to defining the number of sources is to use the available mathematical approaches that aim to identify the number of sources of time period automatically. This is what we did by using MMP in I, II, and III. Other studies have used a method called multiple signal classification (MUSIC) which is based on Eigen value decomposition of data to identify the underlying number of sources of the time-period of EEG data subjected to MUSIC source analysis. These underlying signals after Eigen value decomposition are the so called signal space, and then the entire brain volume is scanned for those source locations that contribute to the signal space. Additional spatiotemporal decomposition approaches such as ICA and SOBI have been proposed (see chapter 5). In I and chapter 5 of this thesis we discuss why these methods are inferior to MMP.

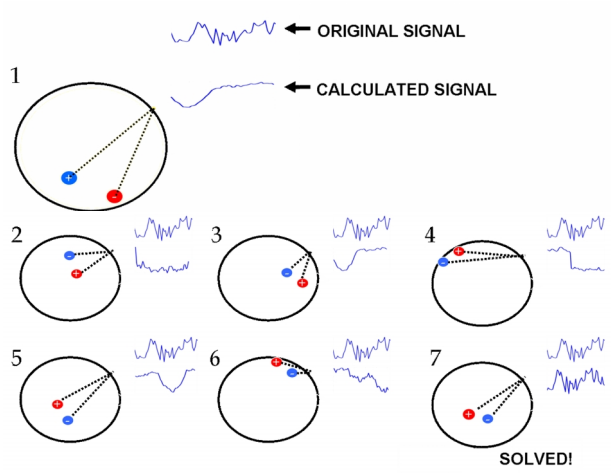

Figure 6. A simplified description of dipolar source modeling. The algorithm finds the source by scanning the brain volume for the source which generates the surface potential with minimal difference from the recorded potentials on the scalp. In this oversimplified example, it took 7 iterations to find the best source.

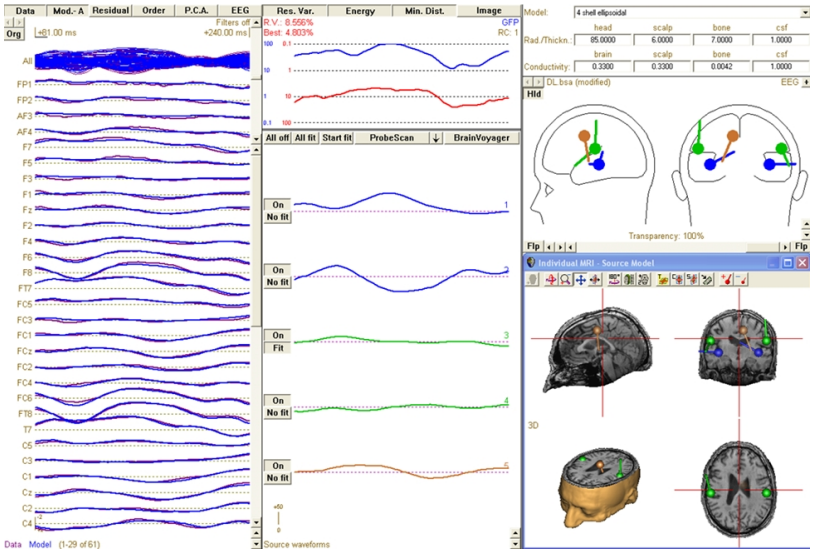

Figure 7. An example from a study done in BESA. This result is from EPs due to pain induced in the rectum in a chronic pancreatitis patient. Left: EP data from all channels. Bottom center: Waveforms of the 5 sources shown to the right of the figure. Top center: grand field power explained by the sources. Top right of the figure: the chosen head model and radius/thickness and conductivity values of each layer. Middle right: Locations of the sources, blue: bilateral insula, green: bilateral SII, brown: cingulate. Bottom right: Brain sources on this individual's MRI scan.

Current density source models: The current density solutions yield blurred source images in contrast to over-focalized point sources as derived by dipole methods. An example of a current density solution is presented in figure 8. The main advantage of current density models over dipolar models is that no á priori assumption about the number of sources is needed. These source models are based on reconstruction of brain electric activity in each point of the 3d grid of solution points, the number of points being much larger than the number of measurement points on the scalp. Each of these solution points can be thought of as current dipoles with fixed positions and varying strength and orientations. The task is to find a unique configuration of activity at each of the points which would explain the measurements recorded on the scalp. However, an infinite number of distributions of current sources within the 3D solution point grid can lead to the same scalp potential map, making this inverse problem highly underdetermined. This means that, some constraints about nature of the source have to be made. In the existing implementations and proposed methods, these constraints are sometimes purely mathematical and sometimes physiological. These constraints are only valid if source distributions fulfilling them are more likely to occur than any other source distribution(Michel, Murray et al., 2004). Regulation parameters are usually introduced to these source solutions to account for the noise in the data and if this parameter is properly defined, then the unexplained part of the data by the inverse solution should correspond to noise. Furthermore, this regulation parameter gives stability to the solution, i.e. small variability in the data should not lead to large variability in the source configuration.

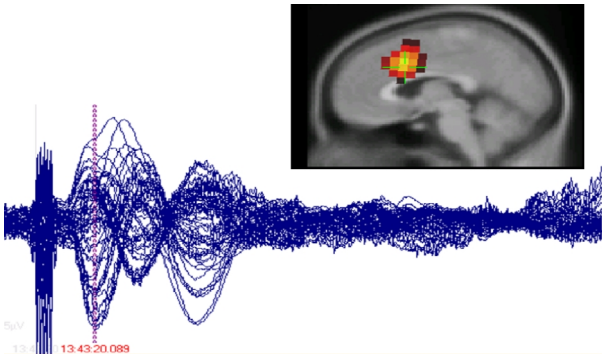

Figure 8. Source localization using a current density method called LORETA as implemented in the CURRY analysis software. The volunteer studied in this figure was stimulated at the pain threshold 30 times at 5Hz in the esophagus while EEG was recorded. Bottom of the figure represents the evoked potential signal of 62 electrodes superimposed on each other. The vertical red line represents the peak under analysis. Top of the figure: LORETA solution around cingulate cortex.

Method	Principles	Discussion
BESA Brain electric source analysis	Fixes the dipole locations over a given time interval and then uses the whole block of data in the least squares fit. The fitting then results in time varying modulation of amplitude of each of these sources.	The technique is very sensitive to the initial guess of the number of dipoles, and therefore it is highly dependent on the level of user expertise. In II and III, we used this method to model the MMP atoms. Since each atom has a single topography describing them, they can usually be modeled by a single dipole and therefore the problem of estimating the number of sources is overcome.
MUSIC Multiple signal classification	Decomposes the data to identify the underlying components (signal space) in the time series. The signal-space is scanned for the optimal number of dipoles. Once they are found, the time course of each individual dipole is determined**.**	This method aims to identify the number of underlying sources automatically. Some of the shortcomings of the original MUSIC with respect to correlated sources in the presence of noise have led to improvements of the original algorithm (i.e. R-MUSIC(Mosher and Leahy, 1998) and RAP-MUSIC(Mosher and Leahy, 1999)). We used R-MUSIC in I in order to model the MMP atoms.
Minimum norm	This method assumes that the 3D current distribution should have a minimum overall intensity(Hamalainen and Ilmoniemi, 1994). It gives a unique solution in the sense that only one combination of sources can at the same time have the lowest overall intensity and exactly fit the scalp data.	The restriction that the overall intensity of the distribution should be minimal is not necessarily physiologically valid. This method favors weak and localized activation patterns. Therefore, this algorithm favors superficial sources because less activity is needed in order to achieve a certain scalp distribution as compared to deep sources. Furthermore, deep sources are incorrectly projected to the surface which can lead to erroneous solutions. Different weighting algorithms have been implemented in order to overcome the drawback of favoring superficial sources (i.e. weighted minimum norm)(Greenblatt, 1993;Gorodnitsky, George et al., 1995;de Peralta-Menendez and Gonzalez-Andino, 1998). However, it must be kept in mind that these approaches are purely mathematical without any physiological justifications for the weights.
LORETA Low-resolution brain electromagnetic tomography	This method selects the solution with a smooth spatial distribution by minimizing the Laplacian of the weighted sources, a measure of spatial roughness. The physiological reasoning behind this constraint is that the activity in neurons in neighboring patches of cortex is correlated(Michel, Murray et al., 2004).	While the assumption that the activity in neurons in neighboring patches of cortex is correlated is correct, the distance between the solution points in 3D grid and the limited spatial resolution of EEG lead to a spatial scale where this assumption is no longer reasonable. Functionally distinct areas can be anatomically very close. As a result, LORETA provides 'over-smoothed' solutions which can include two hemispspheres or different lobes(Fuchs, Wagner et al., 1999;Menendez and Andino, 2000;Trujillo-Barreto, ubert-Vazquez et al., 2004).
Beamformer approaches	Beamformer approaches aim to estimate the activity at one brain site by minimizing the interference of other possible simultaneously active sources(Michel, Murray et al., 2004). The whole brain volume is scanned and the neural activity index is calculated, which describes the activity at a certain location. The sources are assumed to be located at the locations of highest activity index.	Beamformer approaches operate on raw data, instead of averaged data, and therefore induced (and not only evoked) activity can be studied. Beamformers do not need á priori assumption about the number of sources. However, the disadvantage is that these approaches are blind to correlated sources.

Table 1. Description of some of the more commonly used inverse models and their advantages and disadvantages. Dipolar models MUSIC and BESA were used in I, II, and III.

5. Signal decomposition

In order to overcome the mentioned disadvantages of modeling of instantaneous EP data, several signal decomposition methods have been proposed and implemented. One of the most commonly decomposition types applied to EEG is BSS. Another relatively new decomposition approach is the already mentioned MMP method. Both of these approaches are discussed and compared in this chapter.

5.1 Blind source separation

BSS is an approach to estimate and recover the source signals using only the information of their mixtures observed at the recording channels (see figure 9). Blind source separation relies on the assumption that the source signals do not correlate with each other. For example, the signals may be mutually statistically independent or de-correlated. The two most commonly used BSS methods in EEG analysis are ICA and SOBI.

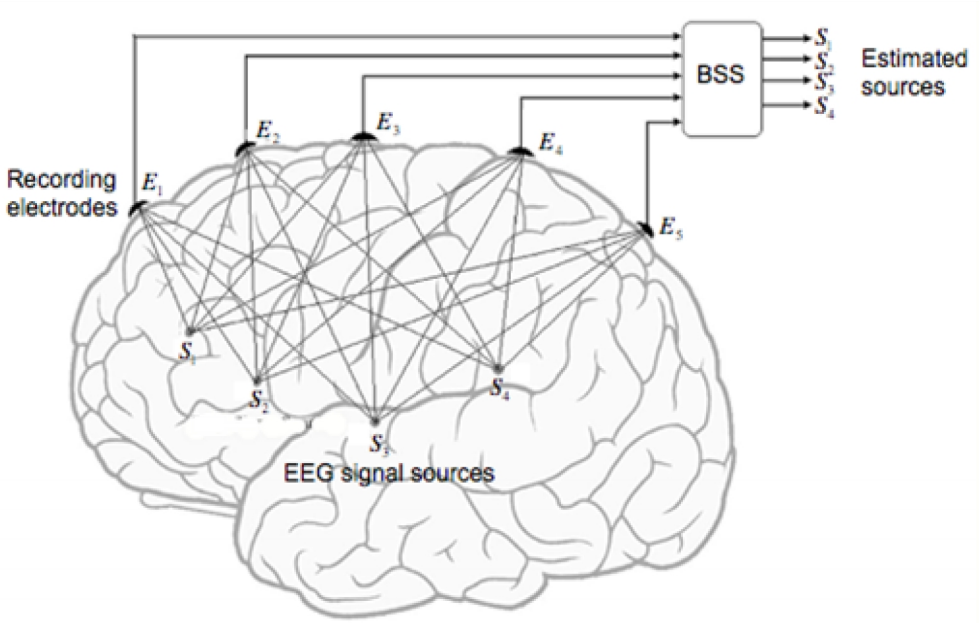

Figure 9. The BSS concept (adapted from (Sanei and Chambers, 2007)). The sources within the brain labeled with S are the generating EEG sources, the black dots labeled with E represent the recording electrodes, and the outputs after the BSS box labeled with S are the estimated sources of signals recorded at the electrodes.

5.1.1 Independent component analysis

ICA is a special case of BSS which is based on the idea of separating a set of components from a signal that is a linear combination of these components, with very little or no knowledge of the component signals. The ICA model can be represented as X=WU, where X is the observed EEG data and both W and U are unknown. Assuming that U is a matrix containing the original components

which are statistically independent, the goal of ICA is to find the mixing matrix W (see figure 10). There are several ways to estimate the mixing matrix W. The infomax ICA algorithm which we used in I is based on maximizing the output entropy(Makeig, Bell et al., 1996). Then W^{-1} is multiplied with the observed signal in order to arrive at the solution for matrix U. The rows of the matrix U are the component activations and the columns are the time points of the input data. The columns of W^{-1} contain the relative projection strengths of each component to each scalp electrode. These projection strengths give the scalp topography of each component and provide evidence for the component's physiological origins, i.e. eye artifacts project to the top, muscle artifacts project to temporal sites, etc(Jung, Makeig et al., 2000). The resulting components are maximally temporally independent and spatially fixed.

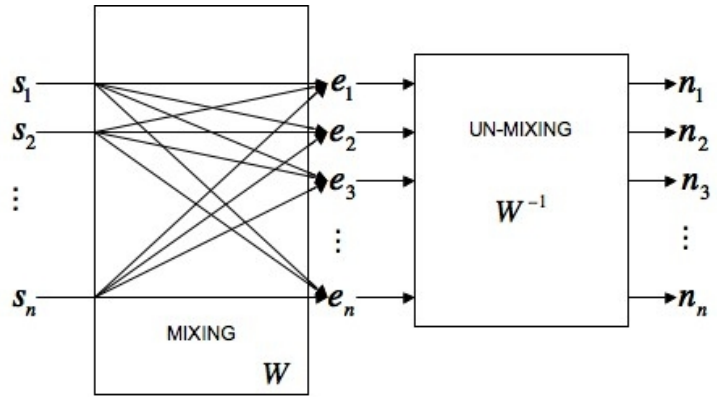

Figure 10. The idea behind Independent component analysis. Each of the sensors e_i (i.e. EEG channels) pick up signals from all of the sources, s_i. The goal of ICA is to find the un-mixing matrix W^{-1} and estimate the original sources, u_i, contributing to the signal picked up by the sensors.

5.1.2 Second order blind identification

SOBI is based on a similar principle as ICA, and uses the same model: X=WU. The main difference between SOBI and ICA lies in how they interpret the data. SOBI exploits second order statistics, while ICA exploits higher order statistics. Higher order statistics exploit statistical independence. This independence is measured by a function of higher order statistics. The restriction is that at most one source can have Gaussian density, because if two sources are Gaussian, it is impossible to distinguish them by using higher order statistics. Second order statistics assume that the sources have different autocorrelation functions. Therefore, such methods are unable to separate processes whose correlations are the same, even when their distributions are different(Even and Moisan, 2005). SOBI exploits the time coherence of the source signals to decompose the mixture of sources. SOBI finds W by minimizing the sum-squared cross-correlations between the components. But, instead of only minimizing the correlation at the same time instant t, SOBI considers cross-correlations at multiple time delays, i.e. between one component at time t and another component at time $t+\tau$ where τ is a time delay(Tang, Liu et al., 2005;Tang, Sutherland et al., 2005). Thus, SOBI takes into account that

one source may affect another at the same time instant or after some temporal delay. These correlations are sensitive to temporal characteristics of the EEG time-series and therefore the temporal information contained in the EEG affects the SOBI results. Therefore, unlike ICA, SOBI it is sensitive to shuffling of data points(Tang, Sutherland et al., 2005).

5.2 Multichannel matching pursuit

MMP is an adaptive and iterative algorithm. It is a generalization of the Matching Pursuit (MP) algorithm(Mallat and Zhang, 1993) for multichannel signals. MP algorithm creates approximations of single-channel signals using a relatively small number of simple components (called atoms) chosen from a very redundant set (called dictionary). Typical components are scaled, translated and modulated Gauss functions and are called Gabor atoms. A very important advantage of such Gabor atoms is their optimal time-frequency localization. The atoms for the approximations are chosen iteratively and adaptively. In the first iteration, the MP algorithm searches the dictionary for a Gabor atom correlated best with the signal under analysis. Next, this atom is subtracted from the signal. This creates the first residuum of the signal. In the second iteration, the MP algorithm searches for a Gabor atom that correlates best with the residuum. By subtracting the atom from the previously computed residuum, the second order residuum is created. This procedure of finding best correlated atoms with the consecutive residues is repeated until the energy of the last computed residuum is below a chosen limit or a number of desired iterations is reached. The result of the MP algorithm is a set of atoms, which summed approximate the signal under analysis. Thanks to the big redundancy of the dictionary, it is possible to create concise approximations with very small number of atoms. The MMP extension of the MP algorithm for multichannel data was presented by Durka(Durka, Matysiak et al., 2005). Briefly, the MMP algorithm searches the dictionary of Gabor atoms for an atom that is correlated best simultaneously with all measurement channels. The sum of the correlation coefficients of a Gabor atom with all data channels is used as a measurement of the global fit of the atom to spatially distributed data. The correlation coefficients define the topographic strength of the Gabor atom in all channels. The Gabor atom together with the list of the correlation coefficients can be treated as a spatio-temporal MMP atom. Such weighted Gabor atom is subtracted from the spatio-temporal data. This creates a spatio-temporal residuum of the data. The next steps follow the MP principle of approximating the consecutive residues. Figure 11 presents MMP decomposition of an artificial multichannel test data containing 4 different spatio-temporal components. The time-frequency properties of the chosen MMP atoms are defined by their base Gabor atoms and the spatial properties are defined by their correlation coefficients. Gabor atoms are completely described by only a few parameters. Thus, the MMP algorithm decomposes multichannel data into simple and parameterized MMP atoms. The chosen atoms are independent from each other in the approximation. The algorithm

keeps the *phase* constant across all channels of MMP atoms. Differences in phase across channels may reveal the direction of information flow between channels. Nonetheless, this flow is credited to a particular single structure. Since this algorithm is meant as a pre-processing step for inverse solutions, it is valid to keep these phases constant and assume that each atom corresponds to the same activity in all the channels(Durka, Matysiak et al., 2005).

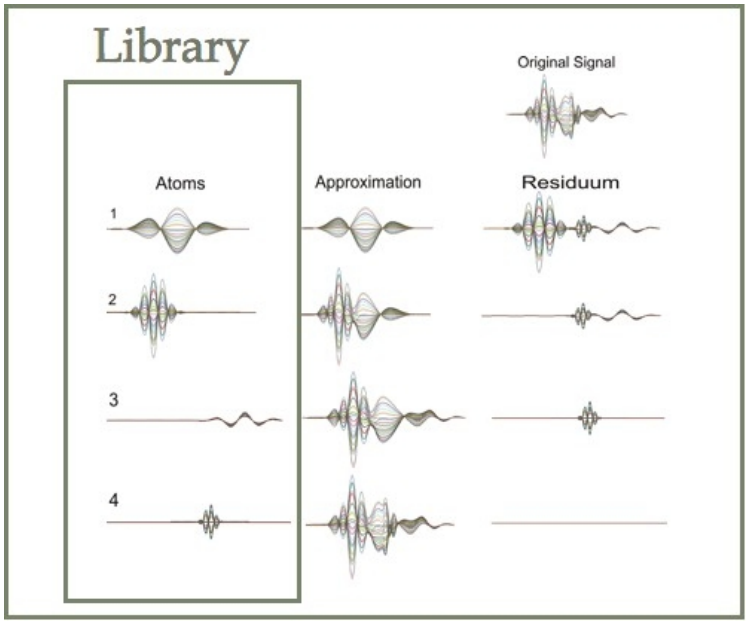

Figure 11. Demonstration of how MMP works. The original signal is shown in the top right corner. Rows 1-4 show the decomposition of the signal. Each row represents one iteration of the MMP algorithm. The atoms column contains the four atoms chosen from the library of atoms. The Approximation column (used for reconstruction purposes) shows the signal approximation when the consecutive atoms are added to each other (e.g., the atoms in line 1 and 2 are added to give the approximation in line 2). Residuum shows the residuum of the signal left after each of the consecutive atoms has been subtracted from it.

5.3 Comparison of MMP to ICA and SOBI and of signal decomposition to raw EP analysis

Both ICA and SOBI are based on statistical analysis of multichannel data. The ICA and SOBI components are time waveforms and factors representing their topographic distribution over the measurement sensors. The MMP atoms are similar to ICA and SOBI components, because MMP atoms can also be seen as waveforms with factors representing spatial distribution. However, the MMP method is not based on statistical analysis and therefore it does not impose any statistical constraints on the data. The MMP atoms chosen for approximation of the data under analysis do not have to be independent. The ICA and SOBI methods tend often to mix activities with different frequencies into a single component. Moreover, they do not provide direct information about the time-frequency distribution of the components. The MMP atoms are mono-frequency components. Single MMP atoms

are completely independent from each other and therefore MMP is able to separate source distributions, which are overlapping in spatial, temporal or frequency domains. Furthermore, MMP provides precise description of time-frequency properties of each atom. Moreover, ICA and SOBI methods are not able to extract the actual number of different sources in the mixed multichannel data. They are able to extract maximally as many components as there are data channels. The real number of signal sources is generally unknown and MMP does not have any constraints on the number of separated components.

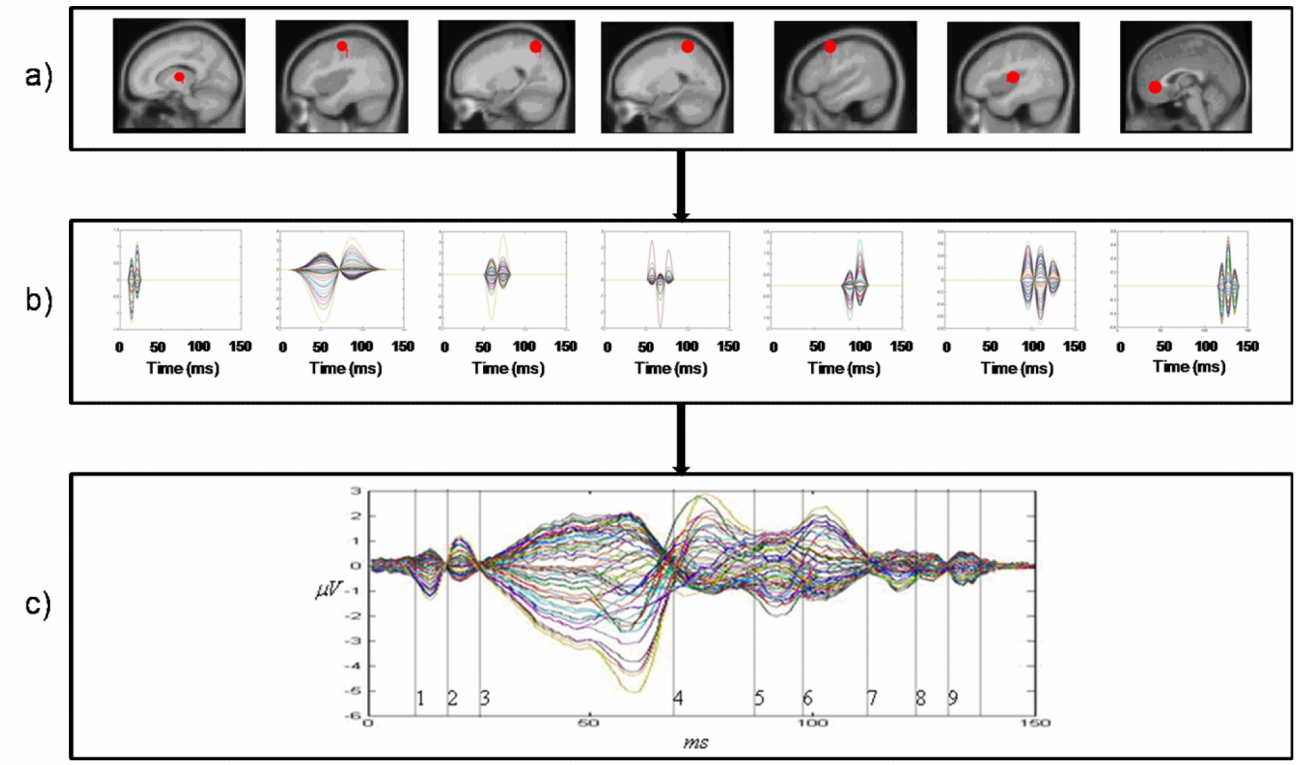

Figure 12. Simulation of EP data (adapted from I); a) placement of six sources in the brain volume: thalamus (dipole 1), SI (dipole 2), bilateral SII (dipoles 3 and 4), pre-motor, insula, and anterior cingulate cortex; b) the simulated waveforms of the brain sources in a); c) the resulting EP after the simulated waveforms were added together and noise with power spectrum of human EEG was added to the sum. The vertical lines mark the time course of the visually extracted peaks. Each number corresponds to a single peak. This evoked potential data was subjected to source localization of each peak and to decomposition by ICA, SOBI, and MMP and source localization of the resulting atoms/components.

In I, we compared the accuracy of MMP decomposition to accuracy of ICA and SOBI decomposition on simulated EP data (see figure 12). We simulated EP data with six dominant brain sources corresponding to the pain matrix (thalamus, SI, bilateral SII, insula, ACC, and pre-motor area). Therefore, this data included both superficial and deep sources and it included waveforms which overlapped in time as seen in the figure. Background noise with power spectrum of human EEG was also added where SNR in dB was defined as, SNR=20*log10(Signal / Noise). We found that MMP

was superior to ICA and SOBI, especially regarding deep and simultaneously active sources. We also compared the source localization of atoms and components to source localization of instantaneous EP data. Source localization of decomposed data was superior to source localization of instantaneous EP data especially regarding the simultaneously active sources. Source localization of MMP atoms was superior to source localization of ICA and SOBI components. Only the superficial sources were correctly recovered in time and location when doing source localization in combination with ICA/SOBI. All the sources were recovered correctly with source localization in combination with MMP (see figure 13 and table 2). Because one particular dataset can be a special case where MMP just happens to be more sensitive to than ICA or SOBI, 20 additional datasets with six dominant sources randomly placed in the brain volume were simulated. We found that source localization in combination with MMP localized 95.9% of the sources <25mm away from the simulated sources and these resulting sources had waveforms which corresponded to the simulations. Whereas, source localization in combination with ICA localized 22.5% of the sources < 25mm away from the simulated sources and source localization in combination with SOBI localized 28.4% of the sources < 25mm away from the simulated sources. Only the waveforms that corresponded to the simulated waveforms were analyzed.

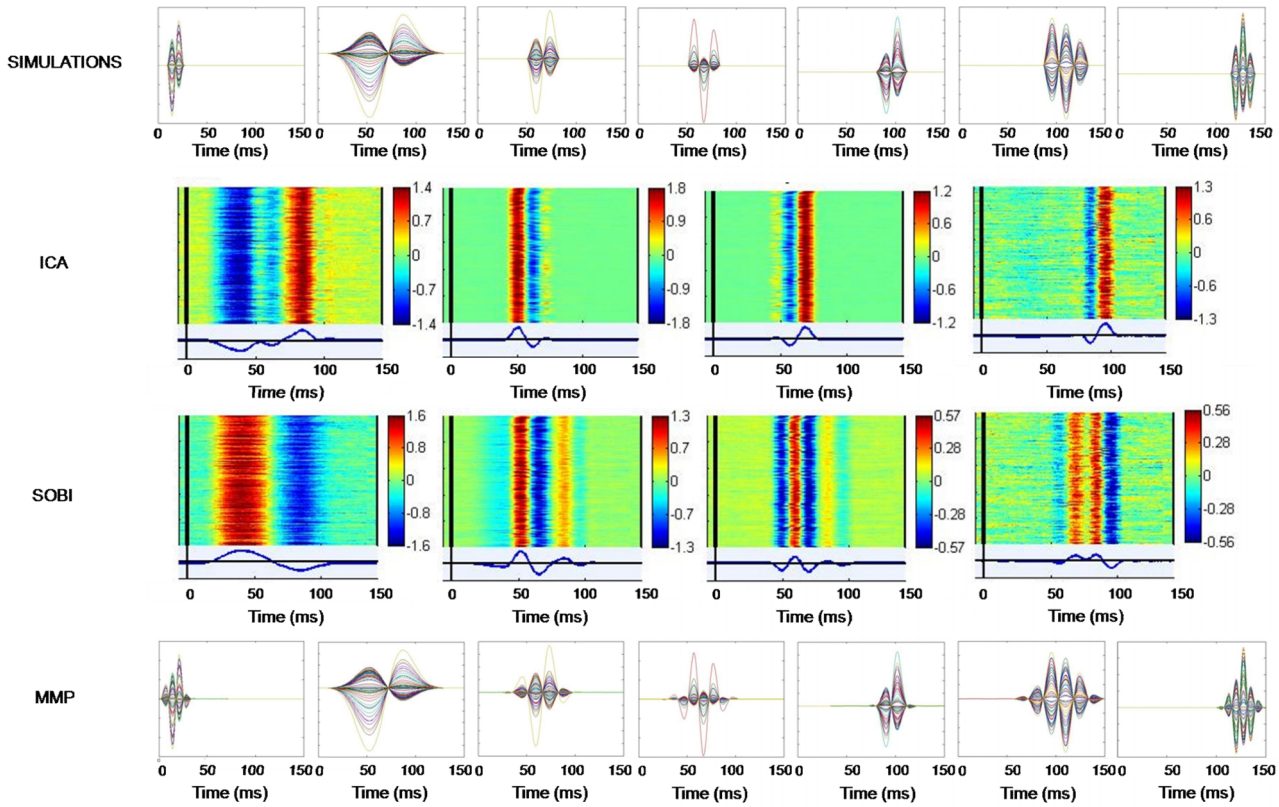

Figure 13. Decomposition results of simulated data (adapted from I). First row represents the original simulations. Second row represents the ICA retrieved components; only four of the simulated components were found correctly, the components 2, 3, 4, and 5 in the first row. Third row represents the SOBI retrieved components; only four of the simulated components were found correctly, the components 2,3,4, and 5 in the first row. Last row represents the MMP retrieved components; all the simulated components were found correctly.

The simulation results were validated on empirical somatosensory EP (SEP) data due to median nerve stimulation. This stimulation paradigm was chosen due to the large consensus in the literature regarding the brain generators of median nerve SEPs. Just as the simulated data, these data were subjected to conventional peak-by-peak source analysis, source analysis on ICA and SOBI components, and source analysis on MMP atoms (figure 14). As can be seen in the figure, ICA and SOBI found three components that were well defined in time with peaks where expected and MMP found five. However, ICA and SOBI components were not as well defined in time as MMP atoms and seem to be composed of several frequencies.

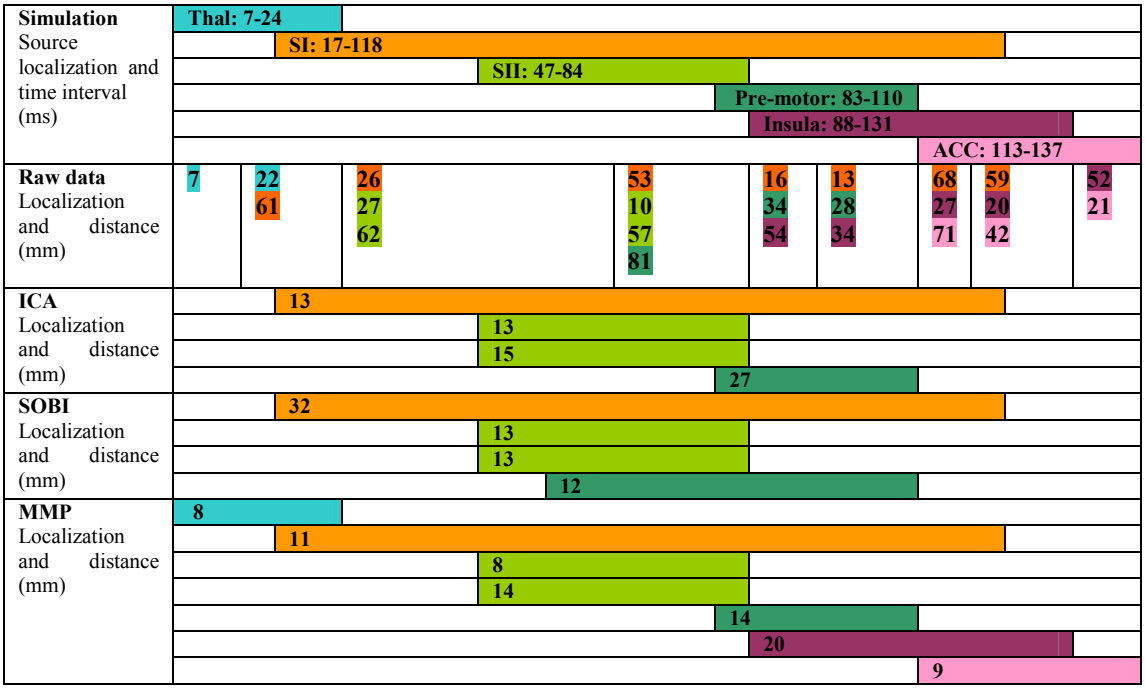

Table 2. Dipole localization results of the raw simulated data and of decomposed simulated data (adapted from I). The first row of the table represents the simulated dipoles. They are color coded according to their location. The length of the color bars indicates the activation time interval of the sources (which is also shown as the numbers representing the ms of activity). In the second row, numbers represent the distance in mm between the calculated dipole for each peak using DIPFIT on the raw data (the 9 numbers in figure 13) and each of the simulated dipoles that were active during that time course. For the raw data there are often many dipoles for each component and the color code depicts the location of the dipole (defined in the simulation row). The third, fourth, and fifth rows represent the anatomical area of the calculated dipole and the distance between the calculated dipole for each of the decomposed components/atoms and the simulated dipole. Abbreviations: Independent Component Analysis (ICA), Second Order Blind Identification (SOBI), Multichannel Matching Pursuit (MMP), Thalamus (Thal), Primary Somatosensory Cortex (SI), Secondary Somatosensory Cortex (SII), Pre-motor (PM), Anterior Cingulate Cortex (ACC).

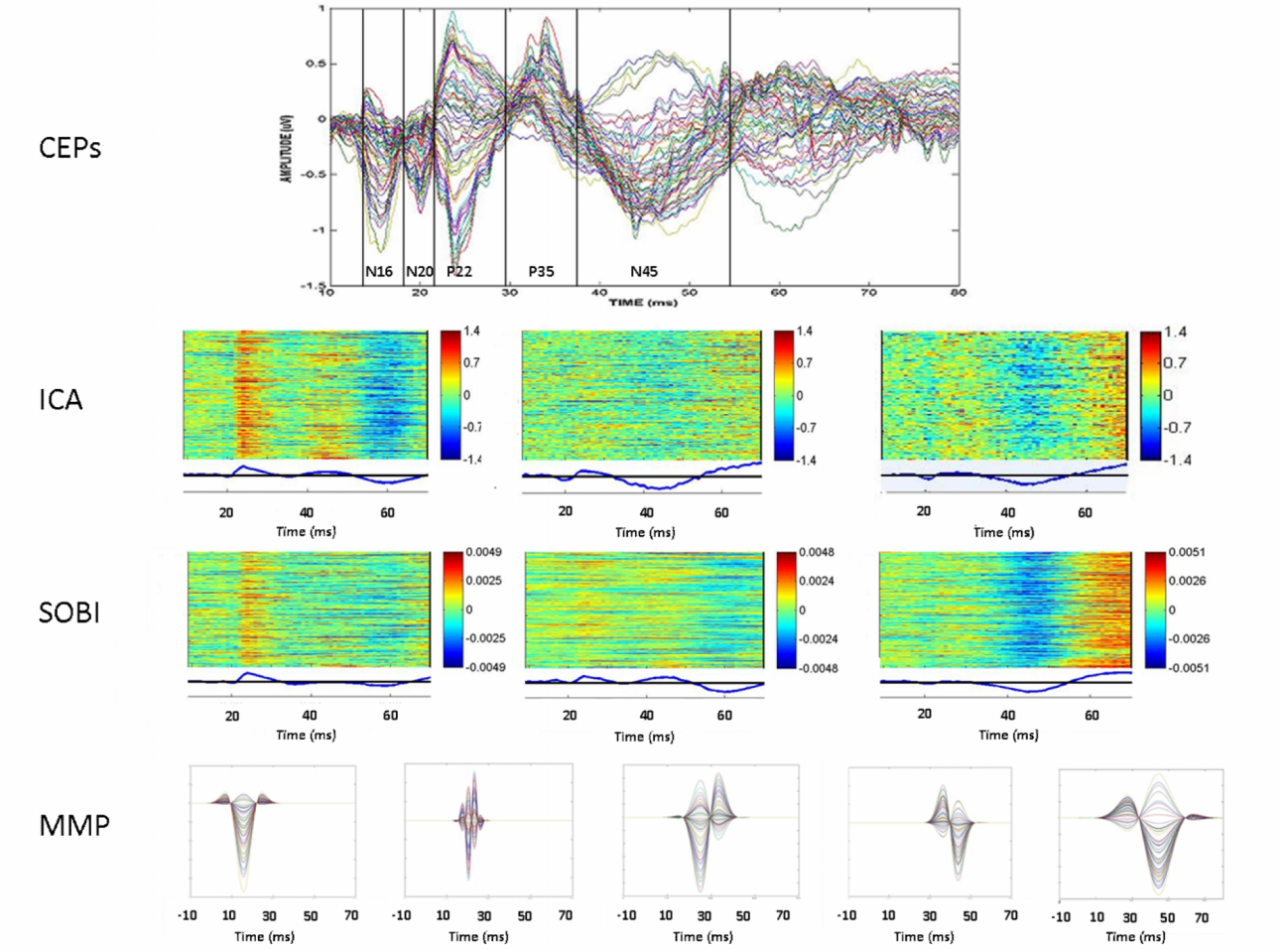

Figure 14. Decomposed median nerve data in one subject (adapted from I). The first row represents the recorded EPs. The peaks that were subjected to inverse modeling are marked by vertical lines. The second row represents the ICA decomposition of the EPs shown in the first row. The third row represents the SOBI decomposition of the EPs shown in the first row. The last row shows the MMP decomposition of the EPs shown in the first row. For all three decomposition methods, the components/atoms that were best defined in time and that had peaks where expected in time are shown.

The detailed discussion of results is found in I. Shortly, decomposing the EPs prior to inverse modeling was superior to inverse modeling on instantaneous EP data. When data were decomposed prior to inverse modeling, it was possible to retrieve simultaneously active dipoles without making any assumptions. The localization of the sources found with localization of decomposed components/atoms corresponds well with the expected brain areas known to be involved in somatosensory processing(Karhu, Hari et al., 1992;Scherg and Buchner, 1993;Spiegel, Tintera et al., 1999;Waberski, Buchner et al., 1999;Valeriani, Le Pera et al., 2000;Valeriani, Le Pera et al., 2001;Arthurs and Boniface, 2003;Thees, Blankenburg et al., 2003;Barba, Valeriani et al., 2005). Although, source localization of MMP atoms found the deeper sources such as the deep subthalamic source at 16ms which was not possible to retrieve with ICA or SOBI. Furthermore, in ICA and SOBI solutions, the

activity seemed rather spread with some visible peaks in several components and finding criterion for component selection from the observed components was not a simple task. Hence, in most cases, it was not apparent which components should be selected just from their event related potentials. By looking at MMP components, on the other hand, it is very easy to choose the most relevant atoms that represent the stimulus triggered activity which deviates from the baseline and background activity because in these atoms the baseline is flat. The atoms corresponding to background (noise) activity are also easily differentiated from the rest of the atoms because they show activity over the entire time interval.

5.4 Limitations of MMP

In the examples presented in the previous section, it was made clear that MMP is superior to ICA and SOBI. However, how far can MMP be pushed? What is the number of sources it can handle? What is the level of noise? This was investigated in II and these questions are answered in this section.

In order to study MMP accuracy as the number of brain sources increases, four different datasets were created. The datasets were divided into simulations of 5, 10, 15, and 20 brain sources. Each of the four datasets included 20 simulations which are described in detail in II. In order to study the accuracy of MMP as the noise level increases, 10 different noise levels were added to the simulations of the four previously created datasets: signal to noise ratios (SNRs) of 20, 16, 14, 10, 6, 2, 1, 0.8, 0.4, and 0.1.

In order to investigate how the accuracy of MMP algorithm is altered with increased number of sources or increased level of noise, all the simulations were decomposed. Then, each of the decomposed atoms was compared to the simulated atoms by using angular separation(Duda, Hart et al., 2001;Teknomo, 2006). If the angular separation between two atoms was ≥ 0.85, the two atoms were deemed as similar.

Figure 15 represents the MMP accuracy results due to increasing number of sources and increasing noise level. Details regarding the results are discussed in II. Briefly, the reasons for the decreased accuracy of source localization due to increased number of sources, as seen in figure 15, are increased complexity, more simultaneously active sources, and more possibilities for the source waveforms to be the same in time, frequency, and phase. It is well known that increased number of sources implies lower stability of inverse solutions(Achim, 1995) and if the complexity of source distribution is too high, the dipole localization can be abandoned for not providing a realistic estimate of the EEG sources(Nunez and Srinivasan, 2006). However, even with this limitation, the MMP method is superior to other more conventional methods regarding the number of simultaneously active sources as demonstrated in I.

Additionally, as seen in figure 15, MMP and source localization of MMP atoms is *robust to noise*. This gives another advantage to source localization in combination with MMP.

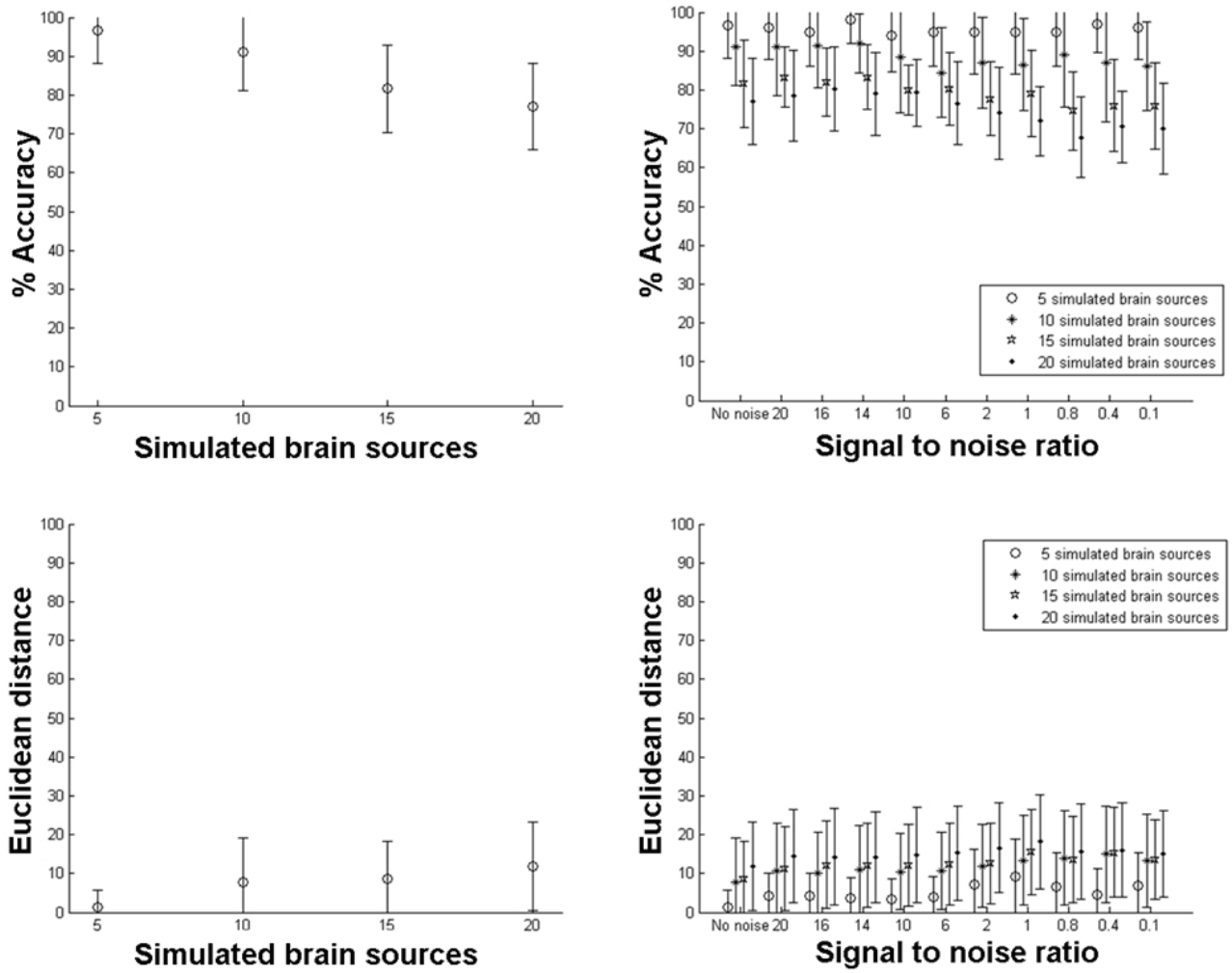

Figure 15. Accuracy of the MMP algorithm (adapted from II). Top left: Accuracy of the MMP atoms' waveforms as the number of brain sources increases. The figure represents the mean and standard deviation of the percent of simulated atoms correctly found after MMP decomposition with 5, 10, 15, and 20 simulated brain sources. Bottom left: brain source localization accuracy of the MMP atoms which had waveforms that corresponded to the simulated brain sources. The figure represents the mean and standard deviation of Euclidean distances between the calculated and simulated brain sources corresponding to simulations with 5, 10, 15, and 20 simulated brain sources. Top right: MMP waveform accuracy as the noise level increases for different number of simulated sources. Bottom right: brain source localization accuracy of the MMP atoms as the noise level increases for different number of simulated sources. The results are ordered from the lowest number of simulated brain sources to the highest.

6. Clustering of multichannel matching pursuit atoms

Typically, MMP followed by source localization is applied to a single subject at a time. This approach makes it difficult to study group differences, i.e. group of patients versus group of healthy controls. As discussed in II, one of the methods to study common sources within a group is grand mean analysis. However, the major shortcoming of this approach is that small differences in brain activation between a few subjects can contaminate the entire solution. Also, grand mean analysis does not allow one to study small differences between individuals and gives a solution that may or may not be representative of the entire population. In order to demonstrate this shortcoming of grand mean analysis, EP data were simulated for ten subjects with 5 dominant sources each (see figure 16). Eight of the subjects contained the exact same sources (both in location and time waveform) and two of the subjects had the same first four sources as the other eight subjects but the fifth source was altered in waveform and location. When taking the grand mean of these 10 subjects (figure 17), a waveform very similar to that of the first 8 subjects is obtained. This is because there are 8 subjects that have the fifth source with a waveform in phase with each other and therefore as these waveforms are averaged, they become bigger in amplitudes and the two different waveforms of subjects 9 and 10 disappear (same principle as when calculating the EPs). Consequently, when this grand mean is decomposed, as seen in figure 17, the atoms retrieved by the decomposition resemble the atoms simulated for subjects 1-8. This method of analysis can lead us to think that these 5 sources are the dominant ones in all the subjects. However, as we can see from figure 17, this is not the case. Therefore, a better method is needed to study similarities/differences between subjects. Another approach is to classify all the differences/similarities between subjects in different groups visually. This process can be tedious and lead to subjective bias, especially when dealing with datasets of many subjects. It would be much better to have a tool to automatically process all the data and output the common features within a group. This method would make it easier to observe any differences or similarities between groups. In II, we proposed a modified K-means clustering procedure to be applied to MMP atoms in a group of subjects in order to automatically study differences/similarities of subjects within a group.

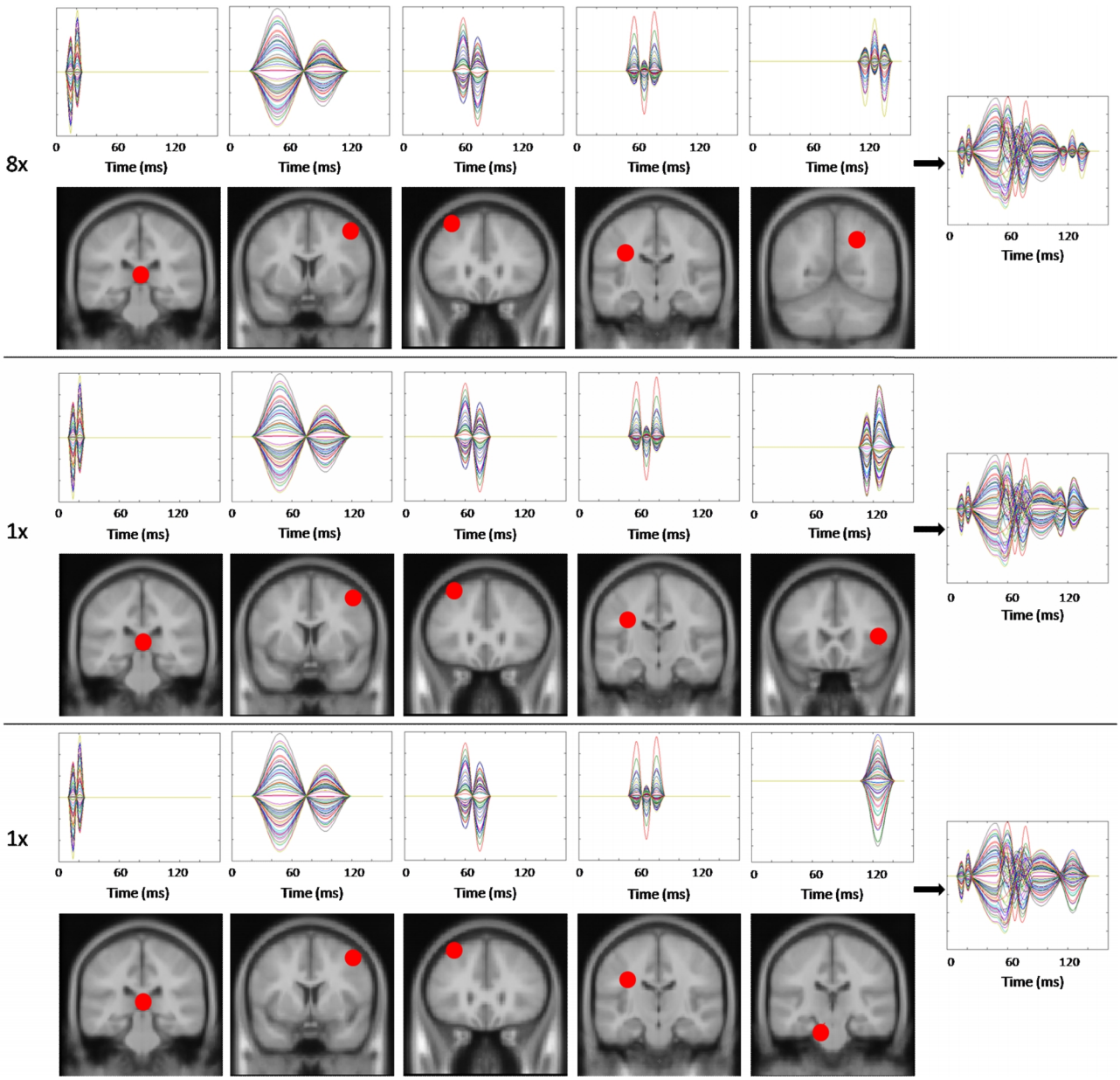

Figure 16. Simulation of evoked potentials in 10 subjects. Top of the figure shows 5 dominant sources in 8 identical simulated subjects: on top are the waveforms and on the bottom are the corresponding sources. To the right of the figure is the evoked potential once these five waveforms are added together. In the middle of the figure is the 9th simulated subject whose first 4 sources are identical to the previous 8 simulated subjects but the 5th source is different in waveform and location. Bottom of the figure shows the 10th simulated subject whose first 4 sources are identical to the previous 9 simulated subjects but the 5th source is different in waveform and location.

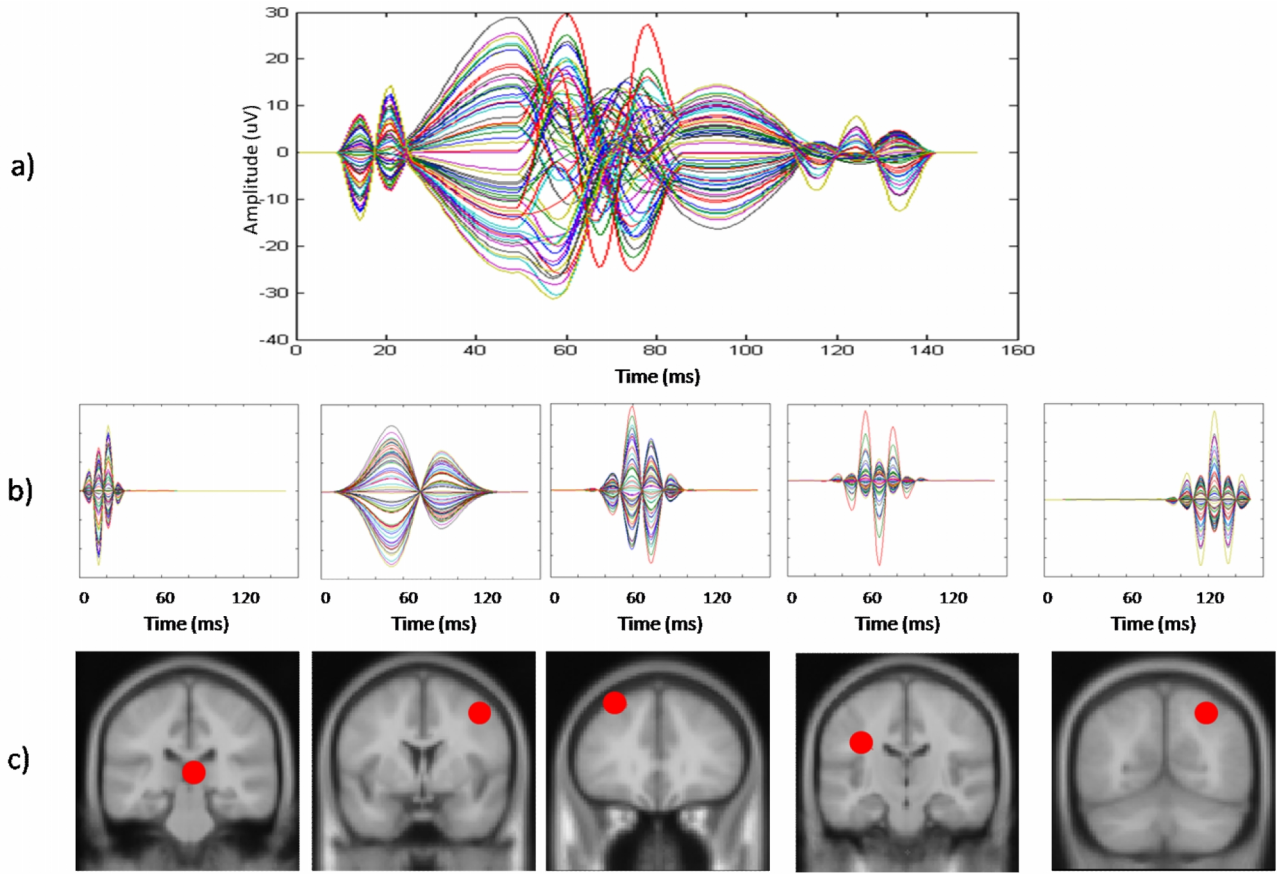

Figure 17. Grand mean analysis of the simulated evoked potentials presented in figure 16: a) grand mean evoked potentials of the simulated 10 subjects. It can be seen that the grand mean very closely resembles the simulated waveform of the first 8 subjects; b) decomposed grand mean. This figure only shows the five atoms that resembled the simulated atoms; c) source localization of the atoms shown in b).

This clustering procedure was applied to the simulated data presented in figure 16 and the results shown in figure 18 were obtained. This time, unlike with the grand mean results in figure 17, it is possible to see that subjects 9 and 10 did not have the 5th atom similar to the rest of the subjects.

The clustering procedure was also successfully applied to SEPs at median nerve and brainstem auditory EPs (BAEP) in II, where the early primary somatosensory cortex activity at 20ms was studied and successfully retrieved for SEPs and the early brainstem activity at 7ms was studied and successfully retrieved for BAEPs.

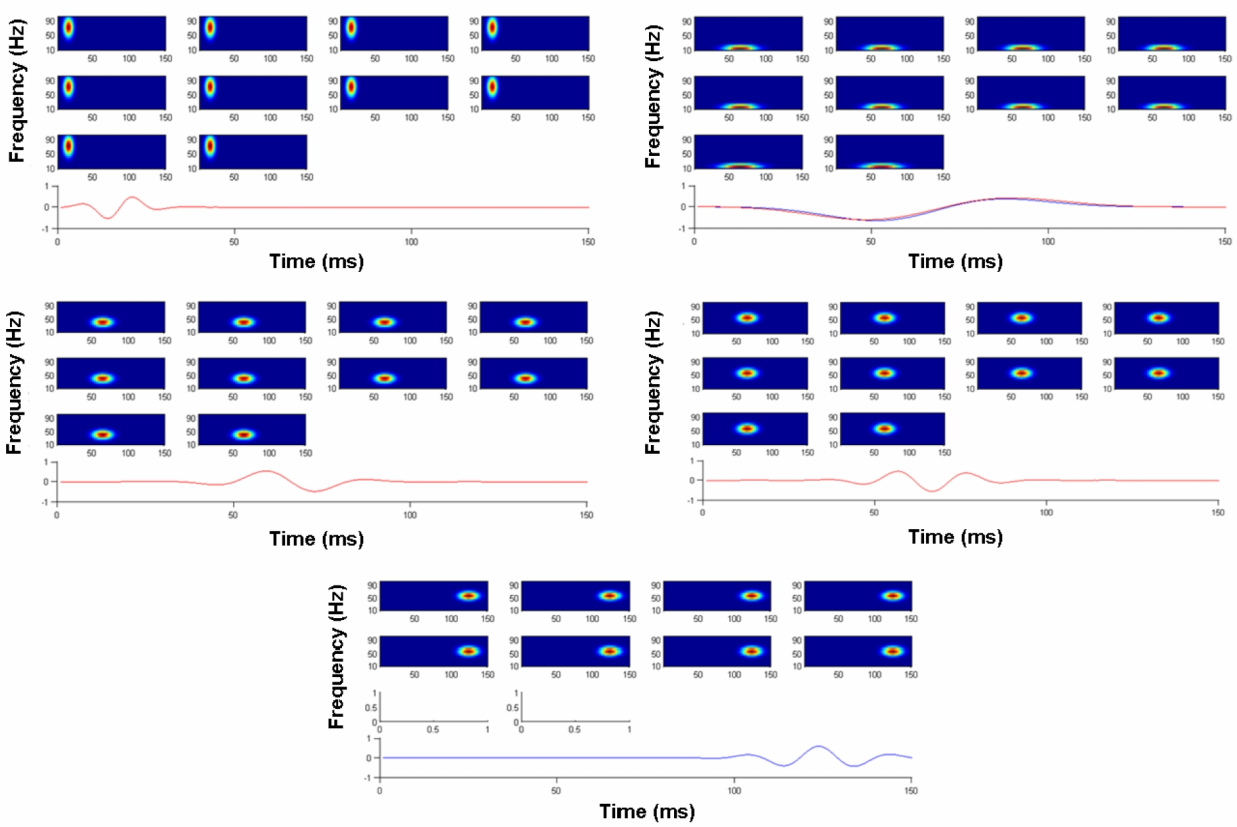

Figure 18. The five clusters representing simulations presented in figure 16. Each of the 5 plots represents a single cluster. In each plot, there are 10 time-frequency subplots representing each subject. The first 4 clusters include atoms from all 10 subjects and the 5th cluster includes atoms from only 8 subjects meaning that the last 2 subjects did not have this atom in their data.

6.1 Limitations of the proposed clustering method

The clustering method proposed in II works well when the time of activity between subjects is similar (i.e. at most a few milliseconds apart). This may not be the case for later "cognitive" potentials like the P300(Nieuwenhuis, Aston-Jones et al., 2005) or N400(Van Petten and Luka, 2006). The identity and time course of activation of such complex event-related potential phenomena may vary greatly across individuals(Moores, Clark et al., 2003). In these cases, the algorithm may be less suitable. This method is mostly suitable for the cases where sources and waveforms between subjects are expected to be similar in time and location, such as in SEPs, visceral EPs, BAEPs, etc.

Since this thesis is concentrated around finding a method for studying of exogenous pain evoked potentials, the clustering method proposed here is very suitable.

7. Bringing it all together: application of multichannel matching pursuit and clustering to pain evoked potentials

The purpose of chapters 1-6 was to discuss shortcomings/advantages of different brain imaging modalities and to give a novel method to be used in the future pain studies to study sequential brain activity due to pain. It was shown that MMP in combination with clustering works well on simulated data and on certain sensory EPs (somatosensory and brainstem auditory). Until this point, in I and II, it was only shown that the method works. However, the question still remains: can these methods be used on biological data that is far more complex than SEPs or BAEPs? In III, we applied the MMP and clustering to EPs due to painful electrical stimulation in the oesophagus before/after placebo/morphine administration (see figure 19). This data was interesting to study with the proposed methods because morphine is the gold standard for treating moderate to severe pain and it is well known that it exerts its primary effect in the central nervous system(Dickenson and Lebars, 1987;Chou, 2009). However, the details of how morphine exerts its effects on the human brain are not well known. Previous human studies have typically looked at PET/fMRI activity in the brain after the placebo/opioid administration. However, as discussed in previous chapters, major disadvantages to these imaging modalities exist, the main one being the inability to follow how the brain activity changes in time on millisecond scale. Previously, recordings with only a few EEG electrodes (≤ 8), typically placed in fronto-central area on the scalp, have mainly been used for determining the analgesic response of opioids(Rohdewald, Granitzki et al., 1988;Kobal, Hummel et al., 1990;Scott, Cooke et al., 1991;Hummel, Hummel et al., 1994;Petersen-Felix, Arendt-Nielsen et al., 1996;Suri, Kaltenbach et al., 1996;Thurauf, Fleischer et al., 1996;Lotsch, Kobal et al., 1997;Quante, Scharein et al., 2004;Chizh, Priestley et al., 2009;Truini, Panuccio et al., 2010) but their results of latencies and amplitudes have shown contradicting values(Banoup, Tetzlaff et al., 2003;Schmidt, Scharein et al., 2007). To our knowledge, only one group did a multichannel EEG (128 channels) study in combination with opioids(Schmidt, Scharein et al., 2007). However, their analysis was limited to latency, amplitude, and topography analysis and therefore still missing the information about alteration of the brain activity due to the drug.

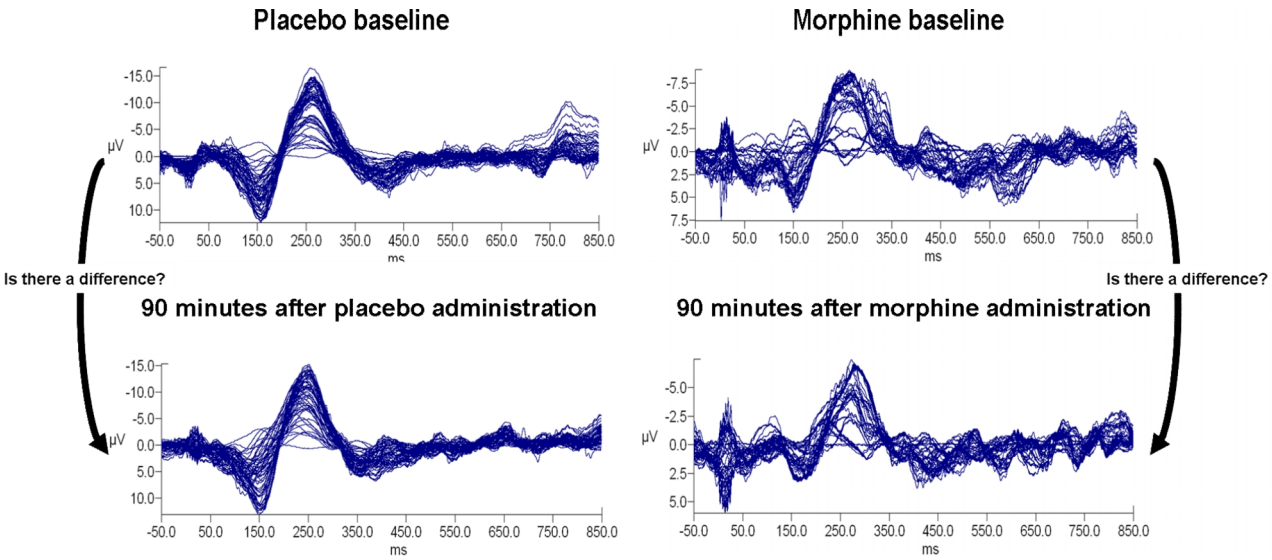

Figure 19. The basic idea of the opioid EP study (adapted from III). The figure shows EPs from 62 channels superimposed on each other due to pain stimulation in esophagus in one subject. Left of the figure are the EPs taken on the day placebo was given and to the right of the figure are EPs taken on the day morphine was given. Top left: EPs before placebo administration. Bottom left: EPs 90 minutes after placebo administration. Top right: EPs before morphine administration. Bottom right: EPs 90 minutes after morphine administration. It was investigated whether there was a change in EPs from before placebo administration to 90 minutes after placebo administration and whether there was a change in EPs from before morphine administration to 90 minutes after morphine administration.

In III, which was a cross-over, double-blinded, placebo controlled study, the methods proposed in I and II were applied as follows:

1. MMP was run on each subject's data.
2. For each subject, atoms with similar time-frequency distributions between baseline and placebo were clustered together. This was done in order to assess how frequency contents changed from baseline to placebo administration in each EEG frequency band.
3. For each subject, atoms with similar time-frequency distributions between baseline and morphine were clustered together. This was done in order to assess how frequency contents changed from baseline to drug administration in each EEG frequency band.
4. Inverse modeling was done on each of the atoms in each cluster in order to assess how brain activity was altered due to placebo/morphine and in which frequency band these changes occurred. The interest was to observe how the brain activity was altered when given two very similar atoms between baseline/placebo or baseline/morphine

We found that the power in EEG delta band decreased due to both placebo and morphine within the first 300 ms and power in beta frequency band decreased only due to morphine after 300 ms (see figures 20 and 21). We found that a trend within the first 300 milliseconds in delta activity was very

apparent as the dipole moved to the frontal left in all subjects after morphine administration. Dipoles due to placebo were reproducible and similar in the two sessions (figures 22 and 23). This finding is very interesting because it is well known that the frontal area of the brain has high density of opioid receptors(Maarrawi, Peyron et al., 2007). Furthermore, it has been shown that stimulation of animal lateral frontal cortex induces analgesia(Oleson, Kirkpatrick et al., 1980;Zhang, Tang et al., 1997). Hence, the fact that we found that the dominant brain activity shifts frontally after administration of morphine is not surprising as it likely reflects activation of the rostral ACC/prefrontal cortex which contain a high concentration of opioid receptors(Willoch, Tolle et al., 1999) and have been suggested as an important region in opioid analgesia(Firestone, Gyulai et al., 1996;Casey, Svensson et al., 2000;Wagner, Willoch et al., 2001;Petrovic, Kalso et al., 2002). Although, the finding is not surprising, and one can say expected, it was now for the first time that we were able to say during which time this shift of activity toward the frontal cortex occurs and moreover in which frequency band: delta, which is known to be the most sensitive for objectifying changes in pain related EPs(Quante, Scharein et al., 2004).

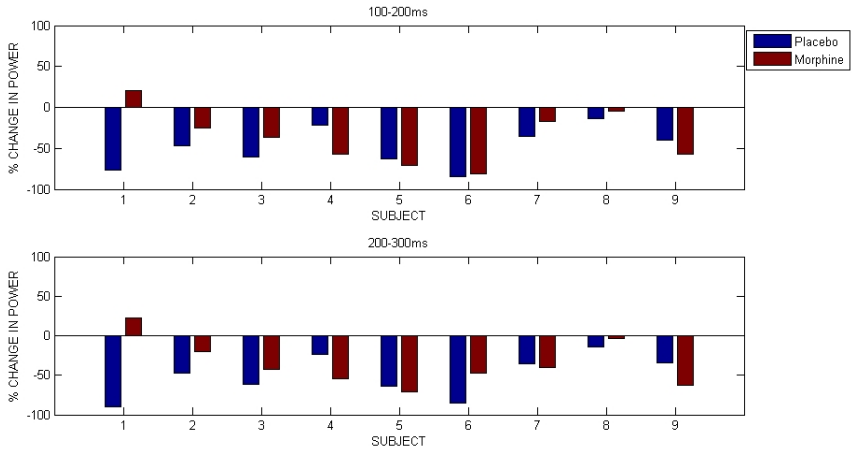

Figure 20. Change in power in delta frequency band (0.5-4Hz) between 100-200 milliseconds and 200-300 milliseconds in all subjects. The decrease in power was significant during these time intervals for placebo and morphine.

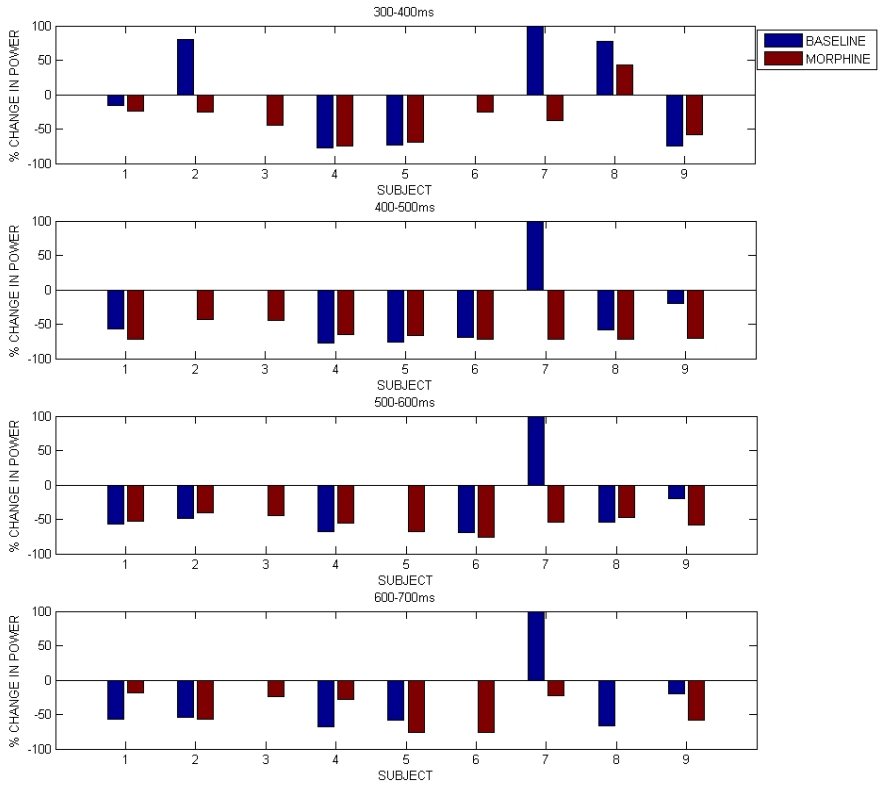

Figure 21. Change in power in beta frequency band (12-30Hz) in all subjects during the following time intervals: 300-400ms, 400-500ms, 500-600ms, and 600-700ms. The decrease in power was significant between 300 and 700 milliseconds for morphine only.

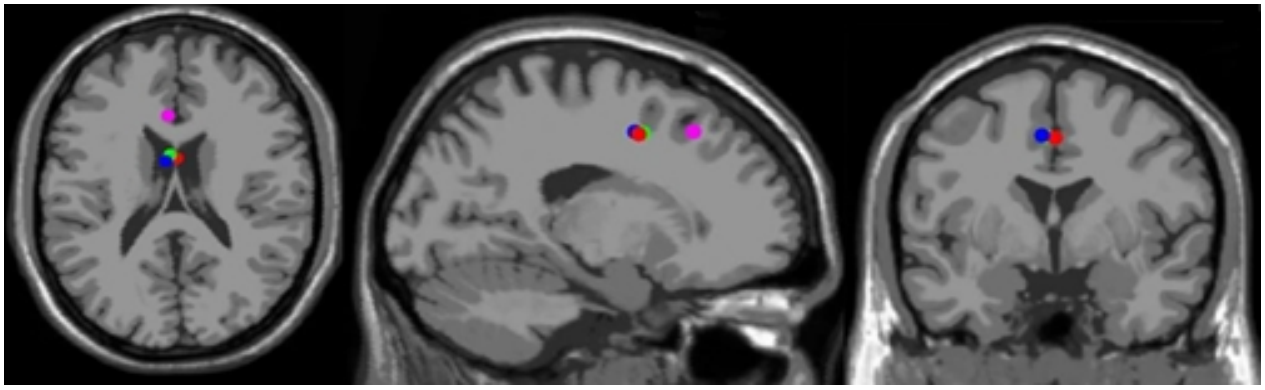

Figure 22. Dipolar source modeling of MMP atoms with delta activity *between 100 and 200 milliseconds* (adapted from III); placebo baseline (green), 90 minutes after placebo administration (blue), morphine baseline (red), and 90 minutes after morphine administration (pink). The results presented in this figure are averages of all subjects' dipoles, although the analysis was done on individuals. Placebo dipoles were reproducible at all coordinates. Dipoles moved frontally and to the left due to morphine.

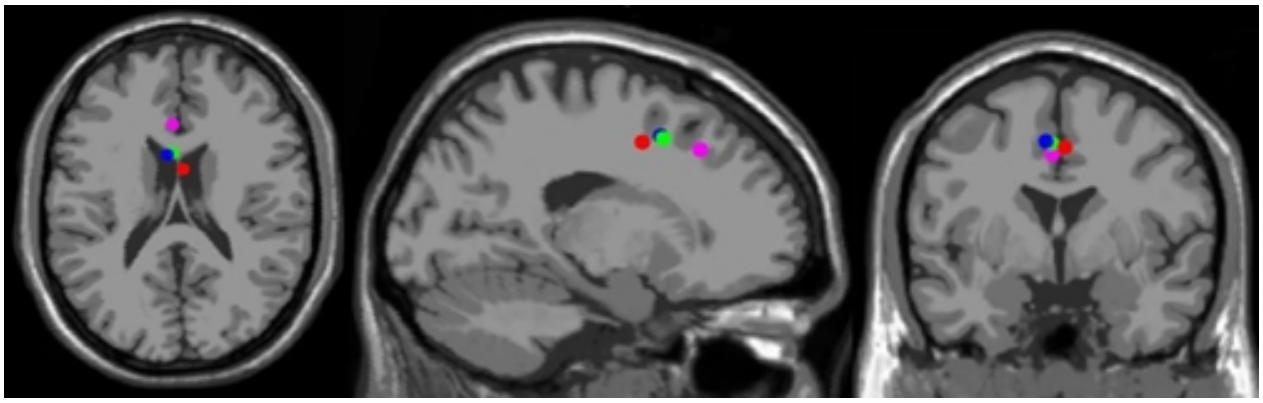

Figure 23. Dipolar source modeling of MMP atoms with delta activity *between 200 and 300 milliseconds* (adapted from III); placebo baseline (green), 90 minutes after placebo administration (blue), morphine baseline (red), and 90 minutes after morphine administration (pink). The results presented in this figure are averages of all subjects' dipoles, although the analysis was done on individuals. Placebo dipoles were reproducible in all coordinates. Dipoles moved frontally and to the left due to morphine.

8. Rectal evoked potentials in constipated patients with rectal hyposensitivity (ongoing study)

Impaired rectal sensation (rectal hyposensitivity (RH)) describes a diminished perception of rectal distension(Wingate, Hongo et al., 2002;Gladman, Lunniss et al., 2006) and is present in one quarter of patients with chronic intractable constipation. The mechanisms contributing to its development are not fully understood. RH may be due to: a) impaired afferent pathway function and/or b) the presence of abnormal rectal wall properties(Gladman, Dvorkin et al., 2005), where it may not necessarily reflect impairment of the afferent nerve pathway. RH as a result of impaired afferent pathway dysfunction may result from disruption at any of the following levels(Gladman, Lunniss et al., 2006): 1) receptor, 2) afferent nerve, or 3) central nervous system. A study done by Gladman et al.(Gladman, Lunniss et al., 2006) showed that 53% of the patients they investigated had normal rectal compliance, adaptation, and tone. These observations support the assumption that the elevation of sensory threshold are not related to alterations in rectal wall properties, but are likely to reflect impairment of afferent nerve function. Cortical representation has never been evaluated in patients with RH and constipation in order to determine whether there is an alteration of central response to stimuli in the rectum. This study aims to demonstrate: 1) feasibility of EPs as a tool to evaluate the integrity of sensory innervations in patients with constipation and RH in comparison to healthy controls, and 2) whether there is cortical reorganization after rectal stimulation in these patients.

Rectal EPs were recorded from 64 surface scalp electrodes in 17 patients and 8 healthy volunteers (ongoing) in response to electrical stimulation of the rectum at 10cm from the anal verge using a specialized bipolar stimulating electrode (4 sets of 50 stimulations, 0.2 Hz frequency, 0.2ms pulse width). Stimuli were delivered at reported pain threshold (VAS=5). Additionally, the sensation threshold (VAS=1) was taken. In order to test for peripheral neuropathy, two series of SEPs after stimulation at median nerve (2 sets of 500 stimulations, 2Hz frequency, 0.2 ms pulse width) were recorded. Additionally, perception thresholds were taken for stimulation at median nerve. All the experiments were carried out at the neurophysiology lab at GI Physiology Unit, Royal London Hospital. Data were analyzed accordingly: 1) sensation thresholds were compared between healthy controls and patients for both median nerve and rectum. 2) Amplitudes and latencies of median nerve SEPs were compared. All of the recording electrodes, superimposed on each other, were looked at and the overall latency and amplitude of each peak were recorded. We looked for the first 7 peaks due to median nerve stimulation which are agreed upon in the literature(Valeriani, Le Pera et al., 2000). 3) SEP topographies were compared for each SEP peak in order to assert that distribution of EEG activity was similar between the two subject groups. 4) Amplitudes and latencies of rectal EPs were compared. The amplitudes and latencies at central (Cz), frontal (FPz), and temporal (T7 and T8) sites were studied. 5) Topographies of rectal EPs were compared.

This was the preliminary analysis of the data. If there are changes in these EP parameters, there are likely changes regarding the generating sources, which will be the final step for analysis of this data.

The sensation thresholds for median nerve were 2.3±0.45 for healthy controls and 2.4±0.67 for RH and constipated patients (*P*=0.5). The thumb twitching thresholds were 7.4±1.33 for healthy controls and 6.25±2.58 for the patients (*P*=0.7). Therefore, there were no significant changes between the healthy controls and the patients for either sensory or motor thresholds. Table 3 shows mean±SD of amplitudes and latencies for median nerve. Furthermore, it shows the *P*-values for comparisons between healthy controls and patients of each peak's latency and amplitude. All the expected EP peaks due to median nerve stimulation were identified in both groups and there were no significant differences between their latencies and amplitudes. The grand mean topographies for each peak are shown in figure 24 and as can be seen that topographies between healthy controls and patients are very similar.

		P14	N20	P25	N35	P45	N65	P90
Latency	Healthy	13.5±0.9	19.7±1.3	26±1.1	35.7±1.1	45.4±3.3	65.1±1.3	95.2±5.3
	Patient	13.5±0.7	19.2±0.6	25.1±0.8	34.1±1.6	45.5±1.8	65±2.5	91±6.1
	P-value	0.5	0.2	0.4	0.8	0.4	0.8	0.5
Amplitude	Healthy	1.3±1.3	1.8±1.3	2.0±3.6	2.1±2.2	2.8±2.4	2.4±2.0	1.8±1.1
	Patient	1.0±0.4	1.7±0.6	1.8±1.9	2.3±1.8	2.6±1.0	1.8±3.3	1.9±0.8
	P-value	0.1	1.0	0.8	0.8	0.7	0.6	0.5

Table 3. Mean±SD values for latencies and amplitudes of the somatosensory evoked potential peaks. The *P*-values show that there are no significant differences in amplitudes of latencies between healthy controls and patients.

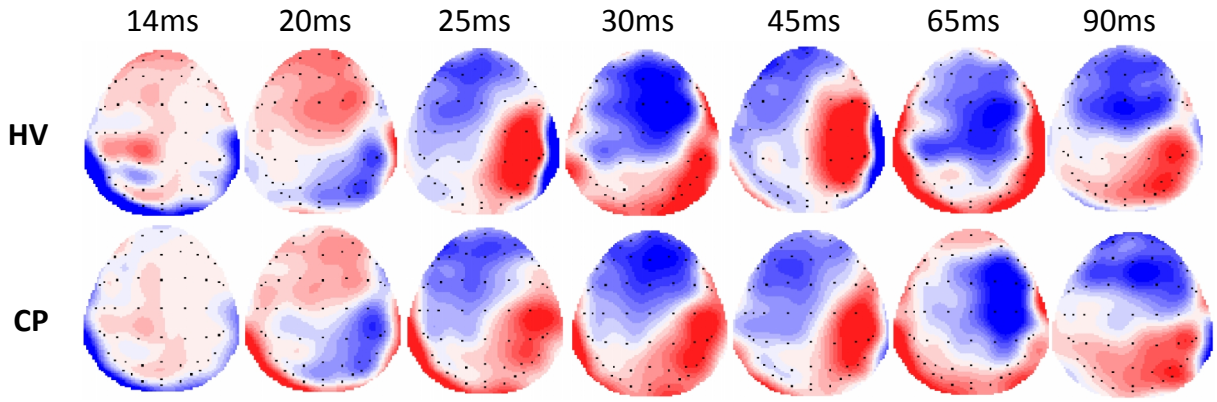

Figure 24. Median nerve topographies at each EP peak for median nerve stimulation for healthy controls and patients. This figure represents the grand mean of all subjects in each group. However, analysis was done on individuals and the individuals fit this model. HV: healthy volunteers, CP: constipated patients.

The sensation thresholds in the rectum were 11±9.09mA for healthy volunteers and 29±20,87mA for RH and constipated patients (P=0.02). The VAS 5 thresholds were 37,5±18,60mA for healthy volunteers and 69±21.74mA for RH and constipated patients (P=0.02). Figure 25 shows grand mean plots of patients versus healthy controls for three electrodes (central (Cz), frontal (FPz), and temporal (T7)). There were no significant differences between amplitudes and latencies in central and temporal electrodes (all $P \geq 0.2$). There were no significant changes in the latency and amplitude of frontal N1 (all $P \geq 0.2$). However, the amplitude of frontal P1 tended to increase in patients (P=0.06). We will likely get a better idea whether this is a significant change or just a trend after performing this experiment in more healthy volunteers. The grand mean topographies of healthy volunteers and patients are shown in figure 26 for N1 and P1. Although, the topographies are similar between healthy controls and patients, the activity in N1 topography seemed to be more spread out over the scalp in patients, while the negativity seemed to dominate very centrally in healthy volunteers.

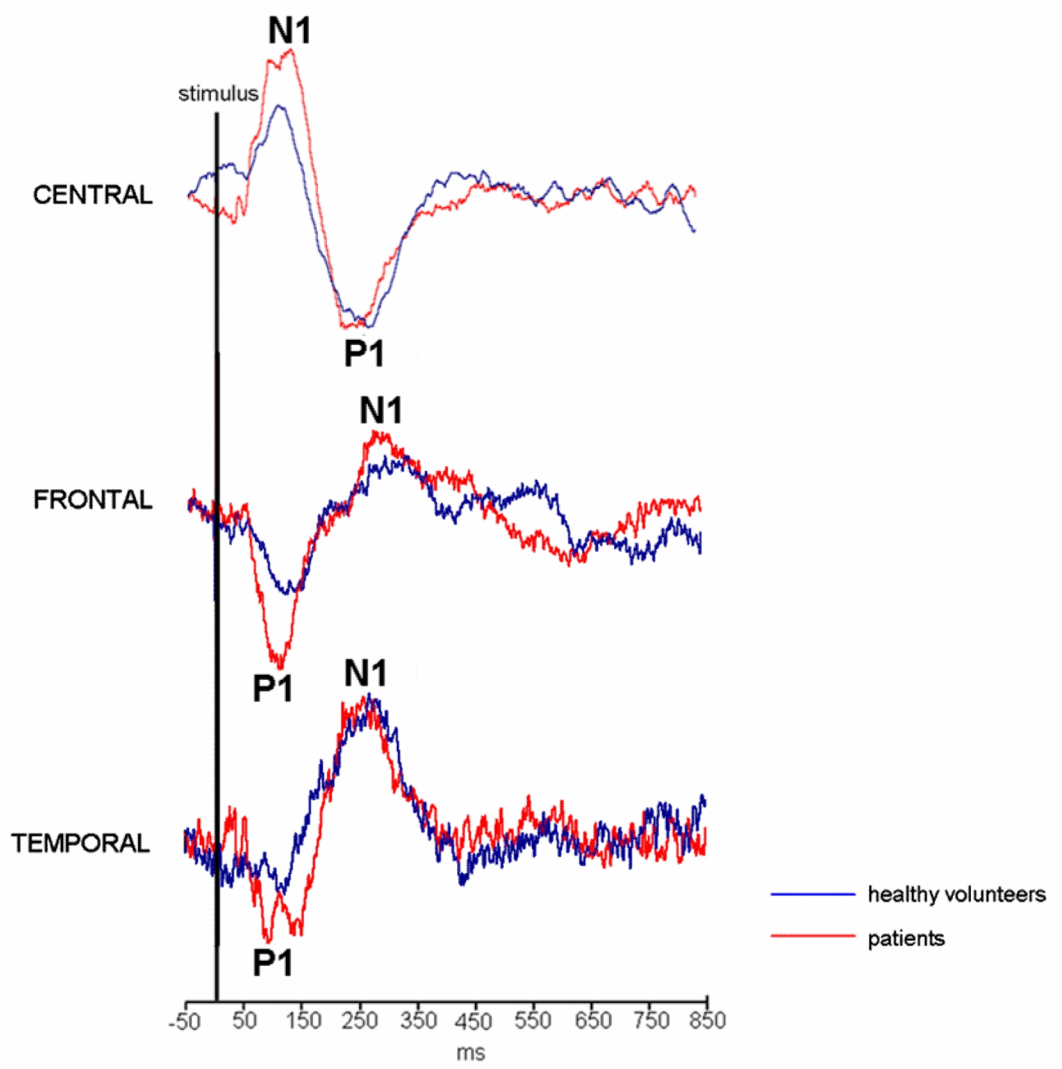

Figure 25. Grand mean averages of the brain evoked potentials from the central (Cz-electrode), frontal (Fz-electrode), and temporal (T7-electrode) regions evoked from painful electrical stimulation in the rectum in rectal hyposensitive constipated patients and healthy volunteers. The early components (N1 and P1) are labelled.

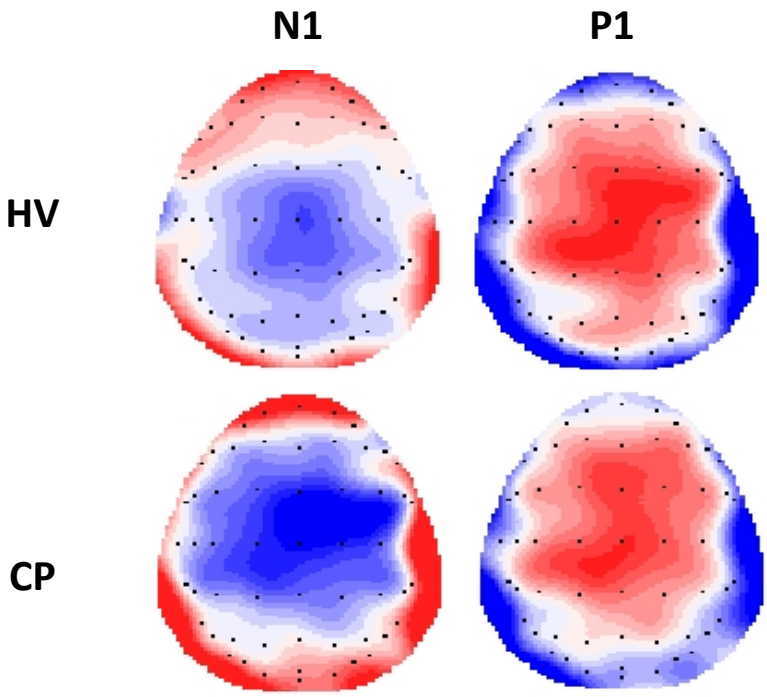

Figure 26. Topographic maps of grand means of N1 and P1 to painful electrical stimulation of the rectum in healthy volunteers and in rectal hyposensitive constipated patients. This figure represents the grand mean of each group. HV: healthy volunteers, CP: constipated patients.

These preliminary results could implicate cortical reorganization in RH and constipated patients. However, once the rest of the data for healthy controls is obtained, it is *crucial* that MMP and source localization analysis be done on individual level because, as previous studies implied, central reorganization could only be present in some types of these patients. If it is the case, in our data, that some of the patients have cortical reorganization, it should be investigated whether there is correlation between these patients and some other data parameters, such as rectum size.

9. Conclusions and future perspectives

This chapter summarizes the conclusions, point by point, of this PhD project.

1. MMP done in combination with inverse modeling is an adequate way to non-invasively estimate brain activity to external stimuli. It is superior to other more conventional decomposition methods such as ICA and SOBI, especially regarding deep and simultaneously active sources.
2. MMP is robust to noise and to limited number of sources (< 10). Even with this limitation, source localization of MMP atoms is superior to source localization of ICA components, SOBI components, or EP peaks.
3. A clustering method was developed in order to automate MMP analysis and more efficiently study differences and similarities between groups.
4. The clustering method proved to be an efficient way to study brain activation sequence and time-frequency distributions of their waveforms within subject groups on simulated data and on SEPs and BAEPs.
5. By applying MMP and clustering to esophageal EP data, it was shown that brain activity moves frontally due to morphine in the first 300 milliseconds after the stimulus. Although, it is well known that activity in the frontal cortex is increased due to morphine, we were able to show during which time interval this shift occurs and in which frequency band. Therefore, the proposed methods were successfully applied to visceral pain evoked potential data and may increase our knowledge on basic mechanisms of how analgesics modify the brain's processing of pain, and provide measures which could be used as powerful biomarkers of analgesia in experimental pain models.
6. Preliminary rectal EP data showed that there may be evidence of central reorganization in constipated patients with RH. However, MMP and source localization need to be applied to the data in order to study how brain activity is altered due to pain in these patients.

9.1 Future Perspectives

MMP and clustering should be used in the future to study differences in brain activity between different groups of subjects, i.e. patients versus healthy controls or in intervention studies investigating e.g., the effect of drugs active on brain activity. Moreover, MMP shall be improved to study single trials instead of the averaged EPs as a lot of time-frequency information is lost in the averaging process.

The patient groups for which the method is intended to be used in the near future are: chronic pancreatitis patients, constipated patients with RH, and diabetes patients in order to study how these patients' brains process pain differently from healthy controls. Furthermore, the methods will be

applied to a new opioid study where 40 healthy volunteers will participate as compared to 12 in study III, to gain a better understanding of how the opioids act on the brain.

All of this combined will eventually lead to the human visceral pain model with brain activation sequence on millisecond scale.

Danish Summary

For at kunne forstå og forbedre smertebehandlingen af patienter, er det nødvendigt at have en forståelse for hjernens bearbejdning af smerter. Størstedelen af vores viden om hjernens bearbejdning af smerter og smertefulde stimuli, er opnået gennem billeddannende studier som f.eks. fMRI og PET skanninger. Den største ulempe ved disse metoder er, at den tidsmæssige opløsning er dårlig. På få millisekunder når de smertedannende signaler fra periferien til hjernen, og det er derfor nødvendigt at anvende metoder med en højere tidsmæssig opløsning end de traditionelle. Evokerede potentialer (EP), som optages via elektroder sat på hovedbunden, måler hjernens aktivitet på en tidsskala hvor enheden er millisekunder, men i modsætning til fMRI og PET har EP ringere rummelig opløsning. Man kan dog ud fra de optagede EP og ved brug af matematiske metoder, beregne hvilke hjernecentre der er aktive under smertefulde stimuli. Dette kaldes ”invers modellering” og anvendes typisk på kontinuerlige EP. Metoden er dog forbundet med en del mangler inklusiv instabilitet ved modellering af især flere og dybe aktive hjernecentre. Ydermere, vil interferens af baggrundsstøj forhindre den optimale beregning af de underliggende aktive hjernecentre.

Denne afhandling, foreslår derfor, i et forsøg på at overvinde manglerne ved de traditionelt anvendte metoder, at de evokerede potentialer dekomposeres, inden anvendelse af matematiske metoder til brug ved invers modellering. Afhandlingen foreslår anvendelse af Multichannel matching pursuit (MMP) som dekomposerings metode. Denne metode har vist sig overlegen i forhold til mere udbredt anvendte dekomposerings metoder som f.eks. independent component analysis (ICA) og second order blind identification (SOBI). MMP har tilmed vist sig overlegen i forhold til anvendelsen af øjeblikkelige EP analyser. Afhandlingen foreslår tilmed en cluster analyse, som også er overlegen i forhold til kontinuerlige EP analyser. Cluster analysen er implementeret og valideret på både simulerede og empiriske somatosensoriske samt og lyd-evokerede potentialer fra hjernestammen. Endeligt er de foreslåede metoder appliceret på EP baseret på viscerale smertestimuleringer for blandt andet at kunne studere morfins effekt i hjernen. De foreslåede metoder har vist sig at være effektive og valide i smertestudier, som involverer evokerede potentialer.

Reference List

Achim A. Cerebral Source Localization Paradigms - Spatiotemporal Source Modeling. Brain and Cognition, 1995; 27: 256-87.

Andersson JLR, Lilja A, Hartvig P, Langstrom B, Gordh T, Handwerker H, Torebjork E. Somatotopic organization along the central sulcus, for pain localization in humans, as revealed by positron emission tomography. Experimental Brain Research, 1997; 117: 192-99.

Apkarian AV, Bushnell MC, Treede RD, Zubieta JK. Human brain mechanisms of pain perception and regulation in health and disease. European Journal of Pain, 2005; 9: 463-84.

Arthurs OJ, Boniface SJ. What aspect of the fMRI BOLD signal best reflects the underlying electrophysiology in human somatosensory cortex? Clinical Neurophysiology, 2003; 114: 1203-09.

Augustine JR. Circuitry and functional aspects of the insular lobe in primates including humans. Brain Research Reviews, 1996; 22: 229-44.

Banoup M, Tetzlaff JE, Schubert A. Pharmacologic and Physiologic Influences Affecting Sensory Evoked Potentials. Anesthesiology, 2003; 99(3): 716-37.

Barba C, Valeriani M, Colicchio G, Mauguiere F. Short and middle-latency Median Nerve (MN) SEPs recorded by depth electrodes in human pre-SMA and SMA-proper. Clinical Neurophysiology, 2005; 116: 2664-74.

Bingel U, Tracey I. Imaging CNS Modulation of Pain in Humans. Physiology, 2008; 23: 371-80.

Breivik H, Collett B, Ventafridda V, Cohen R, Gallacher D. Survey of chronic pain in Europe: Prevalence, impact on daily life, and treatment. European Journal of Pain, 2006; 10: 287-333.

Bromm B, Chen ACN. Brain Electrical Source Analysis of Laser Evoked-Potentials in Response to Painful Trigeminal Nerve-Stimulation. Electroencephalography and Clinical Neurophysiology, 1995; 95: 14-26.

Brooks J, Tracey I. From nociception to pain perception: imaging the spinal and supraspinal pathways. Journal of Anatomy, 2005; 207: 19-33.

Brooks JCW, Nurmikko TJ, Bimson WE, Singh KD, Roberts N. fMRI of thermal pain: Effects of stimulus laterality and attention. Neuroimage, 2002; 15: 293-301.

Buchner H, Fuchs M, Wischmann HA, Dossel O, Ludwig I, Knepper A, Berg P. Source analysis of median nerve and finger stimulated somatosensory evoked potentials: multichannel simultaneous recording of electric and magnetic fields combined with 3D-MR tomography. Brain Topography, 1994; 6: 299-310.

Buchner H, Scherg M. Analysis of the generators of early cortical somatosensory evoked potentials (N. medianus) using dipole source analysis: initial results. EEG-EMG Zeitschrift für Elektroenzephalographie - Elektromyographie und Verwandte Gebiete, 1991; 22: 62-69.

Bushnell MC, Duncan GH, Hofbauer RK, Ha B, Chen JI, Carrier B. Pain perception: is there a role for primary somatosensory cortex? Proceedings of the National Academy of Sciences U. S.A, 1999; 96: 7705-09.

Byers MR, Bonica JJ. Peripheral Pain Mechanisms and Nociceptor Plasticity. In *Bonica's Management of Pain*. Williams & Wilkins: New York, 2001; 26-72.

Casey KL, Minoshima S, Berger KL, Koeppe RA, Morrow TJ, Frey KA. Positron Emission Tomographic Analysis of Cerebral Structures Activated Specifically by Repetitive Noxious Heat Stimuli. Journal of Neurophysiology, 1994; 71: 802-07.

Casey KL, Svensson P, Morrow TJ, Raz J, Jone C, Minoshima S. Selective opiate modulation of nociceptive processing in the human brain. Journal of Neurophysiology, 2000; 84: 525-33.

Chizh BA, Priestley T, Rowbotham M, Schaffler K. Predicting therapeutic efficacy - experimental pain in human subjects. Brain Research Reviews, 2009; 60: 243-54.

Chou R. 2009 Clinical Guidelines from the American Pain Society and the American Academy of Pain Medicine on the use of chronic opioid therapy in chronic noncancer pain: what are the key messages for clinical practice? Polskie Archiwum Medycyny Wewnetrznej-Polish Archives of Internal Medicine, 2009; 119: 469-76.

Chudler EH, Anton F, Dubner R, Kenshalo DR. Responses of Nociceptive SI Neurons in Monkeys and Pain Sensation in Humans Elicited by Noxious Thermal-Stimulation - Effect of Interstimulus-Interval. Journal of Neurophysiology, 1990; 63: 559-69.

Coghill RC, Sang CN, Maisog JH, Iadarola MJ. Pain intensity processing within the human brain: A bilateral, distributed mechanism. Journal of Neurophysiology, 1999; 82: 1934-43.

Coghill RC, Talbot JD, Evans AC, Meyer E, Gjedde A, Bushnell MC, Duncan GH. Distributed-Processing of Pain and Vibration by the Human Brain. Journal of Neuroscience, 1994; 14: 4095-108.

Corbetta M, Miezin FM, Dobmeyer S, Shulman GL, Petersen SE. Selective and Divided Attention During Visual Discriminations of Shape, Color, and Speed - Functional-Anatomy by Positron Emission Tomography. Journal of Neuroscience, 1991; 11: 2383-402.

Davis KD, Kwan CL, Crawley AP, Mikulis DJ. Functional MRI study of thalamic and cortical activations evoked by cutaneous heat, cold, and tactile stimuli. Journal of Neurophysiology, 1998; 80: 1533-46.

Davis KD, Taylor SJ, Crawley AP, Wood ML, Mikulis DJ. Functional MRI of pain- and attention-related activations in the human cingulate cortex. Journal of Neurophysiology, 1997; 77: 3370-80.

De Peralta-Menendez RG, Gonzalez-Andino SL. A critical analysis of linear inverse solutions to the neuroelectromagnetic inverse problem. IEEE Transactions on Biomedical Engineering, 1998; 45: 440-48.

Derbyshire SWG, Jones AKP, Gyulai F, Clark S, Townsend D, Firestone LL. Pain processing during three levels of noxious stimulation produces differential patterns of central activity. Pain, 1997; 73: 431-45.

Derbyshire SWG, Vogt BA, Jones AKP. Pain and Stroop interference tasks activate separate processing modules in anterior cingulate cortex. Experimental Brain Research, 1998; 118: 52-60.

Devinsky O, Morrell MJ, Vogt BA. Contributions of Anterior Cingulate Cortex to Behaviour. Brain, 1995; 118: 279-306.

Dickenson AH, Lebars D. Supraspinal Morphine and Descending Inhibitions Acting on the Dorsal Horn of the Rat. Journal of Physiology-London, 1987; 384: 81-107.

Dimcevski G, Sami SAK, Funch-Jensen P, Le Pera D, Valeriani M, Arendt-Nielsen L, Drewes AM. Pain in chronic pancreatitis: The role of reorganization in the central nervous system. Gastroenterology, 2007; 132: 1546-56.

Dong WK, Chudler EH, Sugiyama K, Roberts VJ, Hayashi T. Somatosensory, Multisensory, and Task-Related Neurons in Cortical Area 7B (Pf) of Unanesthetized Monkeys. Journal of Neurophysiology, 1994; 72: 542-64.

Dong WK, Salonen LD, Kawakami Y, Shiwaku T, Kaukoranta EM, Martin RF. Nociceptive Responses of Trigeminal Neurons in SII-7B Cortex of Awake Monkeys. Brain Research, 1989; 484: 314-24.

Drewes AM, Dimcevski G, Sami SAK, Funch-Jensen P, Huynh KD, Le Pera D, Arendt-Nielsen L, Valeriani M. The "human visceral homunculus" to pain evoked in the oesophagus, stomach, duodenum and sigmoid colon. Experimental Brain Research, 2006; 174: 443-52.

Drewes AM, Gregersen H, Gregersen H, Arendt-Nielsen L. Experimental pain in gastroenterology: A reappraisal of human studies. Scandinavian Journal of Gastroenterology, 2003; 38: 1115-30.

Duda RO, Hart PE, Stork DG. Pattern Classification 510, 2nd ed. Wiley: New York, 2001.

Durka PJ, Matysiak A, Montes EM, Sosa PV, Blinowska KJ. Multichannel matching pursuit and EEG inverse solutions. Journal of Neuroscience Methods, 2005; 148: 49-59.

Even J, Moisan E. Blind source separation using order statistics. Signal Processing, 2005; 85: 1744-58.

Ferretti A, Del Gratta C, Babiloni C, Caulo M, Arienzo D, Tartaro A, Rossini PM, Roman GL. Functional topography of the secondary somatosensory cortex for nonpainful and painful stimulation of median and tibial nerve: an fMRI study. Neuroimage, 2004; 23: 1217-25.

Firestone LL, Gyulai F, Mintun M, Adler LJ, Urso K, Winter PM. Human brain activity response to fentanyl imaged by positron emission tomography. Anesthesia and Analgesia, 1996; 82: 1247-51.

Fitzek S, Fitzek C, Huonker R, Reichenbach JR, Mentzel HJ, Witte OW, Kaiser WA. Event-related fMRI with painful electrical stimulation of the trigeminal nerve. Magnetic Resonance Imaging, 2004; 22: 205-09.

Fuchs M, Wagner M, Kohler T, Wischmann HA. Linear and nonlinear current density reconstructions. Journal of Clinical Neurophysiology, 1999; 16: 267-95.

Gladman MA, Dvorkin LS, Lunniss PJ, Williams NS, Scott SM. Rectal hyposensitivity: A disorder of the rectal wall or the afferent pathway? An assessment using the barostat. American Journal of Gastroenterology, 2005; 100: 106-14.

Gladman MA, Lunniss PJ, Scott SM, Swash M. Rectal hyposensitivity. American Journal of Gastroenterology, 2006; 101: 1140-51.

Gorodnitsky IF, George JS, Rao BD. Neuromagnetic Source Imaging with Focuss - A Recursive Weighted Minimum Norm Algorithm. Electroencephalography and Clinical Neurophysiology, 1995; 95: 231-51.

Gould H. Understanding Pain: What It Is, Why It Happens, and How It's Managed. AAN Press.: St. Paul, MN., 2007.

Greenblatt RE. Probabilistic Reconstruction of Multiple Sources in the Bioelectromagnetic Inverse Problem. Inverse Problems, 1993; 9: 271-84.

Guyton A, Hall J. Textbok of Medical Physiology, 11th ed. Elsevier Saunders: Philadelphia, 2006.

Hamalainen MS, Ilmoniemi RJ. Interpreting Magnetic-Fields of the Brain - Minimum Norm Estimates. Medical & Biological Engineering & Computing, 1994; 32: 35-42.

Hanline B. Back Pain Understood: A Cutting-Edge Approach to Healing Your Back. Medicus Press: 2007.

Hari R, Karhu J, Hamalainen M, Knuutila J, Salonen O, Sams M, Vilkman V. Functional-Organization of the Human 1st and 2nd Somatosensory Cortices - A Neuromagnetic Study. European Journal of Neuroscience, 1993; 5: 724-34.

Hari R, Kaukoranta E, Reinikainen K, Huopaniemie T, Mauno J. Neuromagnetic Localization of Cortical Activity Evoked by Painful Dental Stimulation in Man. Neuroscience Letters, 1983; 42: 77-82.

Hari R, Portin K, Kettenmann B, Jousmaki V, Kobal G. Right-hemisphere preponderance of responses to painful CO2 stimulation of the human nasal mucosa. Pain, 1997; 72: 145-51.

Hennings K, Lelic D, Petrini L. An automated method for micro-state segmentation of evoked potentials. Journal of Neuroscience Methods, 2009; 177: 225-31.

Hobson AR, Furlong PL, Worthen SF, Hillebrand A, Barnes GR, Singh KD, Aziz Q. Real-time imaging of human cortical activity evoked by painful esophageal stimulation. Gastroenterology, 2005; 128: 610-19.

Hummel T, Hummel C, Friedel I, Pauli E, Kobal G. A Comparison of the Antinociceptive Effects of Imipramine, Tramadol and Anpirtoline. British Journal of Clinical Pharmacology, 1994; 37: 325-33.

Huttunen J, Kobal G, Kaukoranta E, Hari R. Cortical Responses to Painful Co2 Stimulation of Nasal-Mucosa - A Magnetoencephalographic Study in Man. Electroencephalography and Clinical Neurophysiology, 1986; 64: 347-49.

Iadarola MJ, Berman KF, Zeffiro TA, Byas-Smith MG, Gracely RH, Max MB, Bennett GJ. Neural activation during acute capsaicin-evoked pain and allodynia assessed with PET. Brain, 1998; 121: 931-47.

Iannetti GD, Mouraux A. From the neuromatrix to the pain matrix (and back). Experimental Brain Research, 2010; 205: 1-12.

Iwata K, Kamo H, Ogawa A, Tsuboi Y, Noma N, Mitsuhashi Y, Taira M, Koshikawa N, Kitagawa J. Anterior Cingulate cortical neuronal activity during perception of noxious thermal stimuli in monkeys. Journal of Neurophysiology, 2005; 94: 1980-91.

Jung TP, Makeig S, Humphries C, Lee TW, McKeown MJ, Iragui V, Sejnowski TJ. Removing electroencephalographic artifacts by blind source separation. Psychophysiology, 2000; 37: 163-78.

Kakigi R, Koyama S, Hoshiyama M, Kitamura Y, Shimojo M, Watanabe S. Pain-Related Magnetic-Fields Following Painful Co2-Laser Stimulation in Man. Neuroscience Letters, 1995; 192: 45-48.

Karhu J, Hari R, Makela JP, Huttunen J, Knuutila J. Cortical Somatosensory Magnetic Responses in Multiple-Sclerosis. Electroencephalography and Clinical Neurophysiology, 1992; 83: 192-200.

Kenshalo DR, Chudler EH, Anton F, Dubner R. SI Nociceptive Neurons Participate in the Encoding Process by Which Monkeys Perceive the Intensity of Noxious Thermal-Stimulation. Brain Research, 1988; 454: 378-82.

Kenshalo DR, Isensee O. Responses of Primate SI Cortical-Neurons to Noxious Stimuli. Journal of Neurophysiology, 1983; 50: 1479-96.

Kobal G, Hummel C, Nuernberg B, Brune K. Effects of Pentazocine and Acetylsalicylic-Acid on Pain-Rating, Pain-Related Evoked-Potentials and Vigilance in Relationship to Pharmacokinetic Parameters. Agents and Actions, 1990; 29: 342-59.

Koles ZJ. Trends in EEG source localization. Electroencephalography and Clinical Neurophysiology, 1998; 106: 127-37.

Krummenacher P, Candia V, Folkers G, Schedlowski M, Schonbachler G. Prefrontal cortex modulates placebo analgesia. Pain, 2010; 148: 368-74.

Lagerlund T, Worrell G. EEG source localization (model-dependent and model-independent methods). In Electroencephalography: basic principles, clinical application, and related fields. Lippincott Williams & Wilkins: Philadelphia, PA, 2005; 829-44.

Lamour Y, Willer JC, Guilbaud G. Rat Somatosensory (SmI) Cortex: I. Characteristics of Neuronal Responses to Noxious-Stimulation and Comparison with Responses to Non-Noxious Stimulation. Experimental Brain Research, 1983; 49: 35-45.

Laurent B, Peyron R, Larrea LG, Mauguiere F. Positron Emission Tomography to study central pain integration. Revue Neurologique, 2000; 156: 341-51.

Lenz FA, Gracely RH, Zirh AT, Romanoski AJ, Dougherty PM. The sensory-limbic model of pain memory - Connections from thalamus to the limbic system mediate the learned component of the affective dimension of pain. Pain Forum, 1997; 6: 22-31.

Liao D, Lelic D, Gao F, Drewes AM, Gregersen H. Biomechanical functional and sensory modelling of the gastrointestinal tract. Philosophical Transactions. Series A, Mathematical, Physical, and Engineering Sciences, 2008; 366: 3281-99.

Lotsch J, Kobal G, Stockmann A, Brune K, Geisslinger G. Lack of analgesic activity of morphine-6-glucuronide after short-term intravenous administration in healthy volunteers. Anesthesiology, 1997; 87: 1348-58.

Maarrawi J, Peyron R, Mertens P, Costes N, Magnin M, Sindou M, Laurent B, Garcia-Larrea L. Motor cortex stimulation for pain control induces changes in the endogenous opioid system. Neurology, 2007; 69: 827-34.

Makeig S, Bell A, Jung TP, Sejnowski TJ. Independent Component Analysis of Electroencephalographic Data. Advances in Neural Information Processing Systems, 1996; 8: 145-51.

Mallat SG, Zhang ZF. Matching Pursuits with Time-Frequency Dictionaries. IEEE Transactions on Signal Processing, 1993; 41: 3397-415.

Malmivuo J, Plonsey R. Bioelectromagnetism: principles and applications of bioelectric and biomagnetic fields. Oxford University Press: New York, 1995.

Martin JH. The collective electrical behavior of cortical neurons: the electroencephalogram and the mechanisms of epilepsy. In Principles of Neural Science. Norwalk: Appleton and Lange: 1991; 777-91.

Menendez RGD, Andino SLG. Discussing the capabilities of Laplacian Minimization. Brain Topography, 2000; 13: 97-104.

Michel CM, Murray MM, Lantz G, Gonzalez S, Spinelli L, de Peralta RG. EEG source imaging. Clinical Neurophysiology, 2004; 115: 2195-222.

Mohr C, Binkofski F, Erdmann C, Buchel C, Helmchen C. The anterior cingulate cortex contains distinct areas dissociating external from self-administered painful stimulation: a parametric fMRI study. Pain, 2005; 114: 347-57.

Moores KA, Clark CR, Hadfield JLM, Brown GC, Taylor DJ, Fitzgibbon SP, Lewis AC, Weber DL, Greenblatt R. Investigating the generators of the scalp recorded visuo-verbal P300 using cortically constrained source localization. Human Brain Mapping, 2003; 18: 53-77.

Mosher JC, Leahy RM. Recursive MUSIC: A framework for EEG and MEG source localization. IEEE Transactions on Biomedical Engineering, 1998; 45: 1342-54.

Mosher JC, Leahy RM. Source localization using recursively applied and projected (RAP) MUSIC. IEEE Transactions on Signal Processing, 1999; 47: 332-40.

Mosher JC, Lewis PS, Leahy RM. Multiple Dipole Modeling and Localization from Spatiotemporal MEG Data. IEEE Transactions on Biomedical Engineering, 1992; 39: 541-57.

Nieuwenhuis S, Aston-Jones G, Cohen JD. Decision making, the p3, and the locus coeruleus-norepinephrine system. Psychological Bulletin, 2005; 131: 510-32.

Nunez PL, Srinivasan R. Electric fields of the brain: the neurophysics of EEG, 2nd ed. Oxford University Press: New York, 2006.

Olesen SS, Frøkjær JB, Lelic D, Valeriani M, Drewes AM. Altered cerebral pain processing in chronic pancreatitis. Pancreatology, 2010; 10(6): 742-51.

Oleson TD, Kirkpatrick DB, Goodman SJ. Elevation of pain threshold to tooth shock by brain stimulation in primates. Brain Research, 1980; 194: 79-95.

Pazzaglia C, Valeriani M. Brain-evoked potentials as a tool for diagnosing neuropathic pain. Expert Review of Neurotherapeutics, 2009; 9: 759-71.

Petersen SE, Fox PT, Posner MI, Mintun M, Raichle ME. Positron Emission Tomographic Studies of the Cortical Anatomy of Single-Word Processing. Nature, 1988; 331: 585-89.

Petersen-Felix S, Arendt-Nielsen L, Bak P, Fischer M, Zbinden AM. Psychophysical and electrophysiological responses to experimental pain may be influenced by sedation: comparison of the effects of a hypnotic (propofol) and an analgesic (alfentanil). British Journal of Anaesthesia, 1996; 77: 165-71.

Petrovic P, Kalso E, Petersson KM, Ingvar M. Placebo and opioid analgesia - Imaging a shared neuronal network. Science, 2002; 295: 1737-40.

Ploner M, Freund HJ, Schnitzler A. Pain affect without pain sensation in a patient with a postcentral lesion. Pain, 1999; 81: 211-14.

Ploner M, Schmitz F, Freund HJ, Schnitzler A. Differential organization of touch and pain in human primary somatosensory cortex. Journal of Neurophysiology, 2000; 83: 1770-76.

Ploner M, Schmitz F, Freund HJ, Schnitzler A. Parallel activation of primary and secondary somatosensory cortices in human pain processing. Journal of Neurophysiology, 1999; 81: 3100-04.

Ploner M, Schnitzler A. Cortical representation of pain. Nervenarzt, 2004; 75: 962-9.

Price DD. Neuroscience - Psychological and neural mechanisms of the affective dimension of pain. Science, 2000; 288: 1769-72.

Quante M, Scharein E, Zimmermann R, Langer-Brauburger B, Bromm B. Dissociation of morphine analgesia and sedation evaluated by EEG measures in healthy volunteers. Arzneimittel-Forschung, 2004; 54: 143-51.

Rainville P, Duncan GH, Price DD, Carrier B, Bushnell MC. Pain affect encoded in human anterior cingulate but not somatosensory cortex. Science, 1997; 277: 968-71.

Rohdewald P, Granitzki HW, Neddermann E. Comparison of the analgesic efficacy of metamizole and tramadol in experimental pain. Pharmacology, 1988; 37: 209-17.

Sanei S, Chambers JA. EEG Signal Processing. John Wiley & Sons, Ltd: 2007.

Schaul N. The fundamental neural mechanisms of electroencephalography. Electroencephalography and Clinical Neurophysiology, 1998; 106: 101-07.

Scherg M, Bast T, Berg P. Multiple source analysis of interictal spikes: Goals, requirements, and clinical value. Journal of Clinical Neurophysiology, 1999; 16: 214-24.

Scherg M, Buchner H. Somatosensory-Evoked Potentials and Magnetic-Fields - Separation of Multiple Source Activities. Physiological Measurement, 1993; 14: A35-A39.

Schmidt GN, Scharein E, Siegel M, Muller J, Debener S, Nitzschke R, Engel A, Bischoff P. Identification of sensory blockade by somatosensory and pain-induced evoked potentials. Anesthesiology, 2007; 106: 707-14.

Schnitzler A, Ploner M. Neurophysiology and functional neuroanatomy of pain perception. Journal of Clinical Neurophysiology, 2000; 17: 592-603.

Schnitzler A, Volkmann J, Enck P, Frieling T, Witte OW, Freund HJ. Different cortical organization of visceral and somatic sensation in humans. European Journal of Neuroscience, 1999; 11: 305-15.

Scott JC, Cooke JE, Stanski DR. Electroencephalographic Quantitation of Opioid Effect - Comparative Pharmacodynamics of Fentanyl and Sufentanil. Anesthesiology, 1991; 74: 34-42.

Sharma A, Lelic D, Brock C, Paine P, Aziz Q. New technologies to investigate the brain-gut axis. World Journal of Gastroenterology, 2009; 15: 182-91.

Shi CJ, Cassell MD. Cascade projections from somatosensory cortex to the rat basolateral amygdala via the parietal insular cortex. Journal of Comparative Neurology, 1998a; 399: 469-91.

Shi CJ, Cassell MD. Cortical, thalamic, and amygdaloid connections of the anterior and posterior insular cortices. Journal of Comparative Neurology, 1998b; 399: 440-68.

Sikes RW, Vogt LJ, Vogt BA. Distribution and properties of visceral nociceptive neurons in rabbit cingulate cortex. Pain, 2008; 135: 160-74.

Spiegel J, Hansen C, Treede RD. Laser-evoked potentials after painful hand and foot stimulation in humans: Evidence for generation of the middle-latency component in the secondary somatosensory cortex. Neuroscience Letters, 1996; 216: 179-82.

Spiegel J, Tintera J, Gawehn J, Stoeter P, Treede RD. Functional MRI of human primary somatosensory and motor cortex during median nerve stimulation. Clinical Neurophysiology, 1999; 110: 47-52.

Staahl C, Reddy H, Andersen SD, Arendt-Nielsen L, Drewes AM. Multi-modal and tissue-differentiated experimental pain assessment: Reproducibility of a new concept for assessment of analgesics. Basic & Clinical Pharmacology & Toxicology, 2006; 98: 201-11.

Stevens RT, London SM, Apkarian AV. Spinothalamocortical Projections to the Secondary Somatosensory Cortex (SII) in Squirrel-Monkey. Brain Research, 1993; 631: 241-46.

Suri A, Kaltenbach ML, Grundy BL, Derendorf H. Pharmacodynamic evaluation of codeine using tooth pulp evoked potentials. Journal of Clinical Pharmacology, 1996; 36: 1126-31.

Talbot JD, Marrett S, Evans AC, Meyer E, Bushnell MC, Duncan GH. Multiple Representations of Pain in Human Cerebral-Cortex. Science, 1991; 251: 1355-58.

Tang AC, Liu JY, Sutherland MT. Recovery of correlated neuronal sources from EEG: The good and bad ways of using SOBI. Neuroimage, 2005; 28: 507-19.

Tang AC, Sutherland MT, McKinney CJ. Validation of SOBI components from high-density EEG. Neuroimage, 2005; 25: 539-53.

Tarkka IM, Treede RD. Equivalent Electrical Source Analysis of Pain-Related Somatosensory-Evoked Potentials Elicited by A Co2-Laser. Journal of Clinical Neurophysiology, 1993; 10: 513-19.

Teknomo K. Similarity Measurement. http://people.revoledu.com/kardi/tutorial/Similarity, 2006.

Thees S, Blankenburg F, Taskin B, Curio G, Villringer A. Dipole source localization and fMRI of simultaneously recorded data applied to somatosensory categorization. Neuroimage, 2003; 18: 707-19.

Thurauf N, Fleischer WK, Liefhold J, Schmid O, Kobal G. Dose dependent time course of the analgesic effect of a sustained-release preparation of tramadol on experimental phasic and tonic pain. British Journal of Clinical Pharmacology, 1996; 41: 115-23.

Torquati K, Pizzella V, Della Penna S, Franciotti R, Babiloni C, Rossini PM, Romani GL. Comparison between SI and SII responses as a function of stimulus intensity. Neuroreport, 2002; 13: 813-19.

Treede RD, Jensen TS, Campbell JN, Cruccu G, Dostrovsky JO, Griffin JW, Hansson P, Hughes R, Nurmikko T, Serra J. Neuropathic pain - Redefinition and a grading system for clinical and research purposes. Neurology, 2008; 70: 1630-35.

Truini A, Panuccio G, Galeotti F, Maluccio MR, Sartucci F, Avoli M, Cruccu G. Laser-evoked potentials as a tool for assessing the efficacy of antinociceptive drugs. European Journal of Pain, 2010; 14: 222-25.

Trujillo-Barreto NJ, Aubert-Vazquez E, Valdes-Sosa PA. Bayesian model averaging in EEG/MEG imaging. Neuroimage, 2004; 21: 1300-19.

Valeriani M, Le Pera D, Niddam D, Arendt-Nielsen L, Chen ACN. Dipolar source modeling of somatosensory evoked potentials to painful and nonpainful median nerve stimulation. Muscle & Nerve, 2000; 23: 1194-203.

Valeriani M, Le Pera D, Tonali P. Characterizing somatosensory evoked potential sources with dipole models: Advantages and limitations. Muscle & Nerve, 2001; 24: 325-39.

Van Petten C, Luka BJ. Neural localization of semantic context effects in electromagnetic and hemodynamic studies. Brain and Language, 2006; 97: 279-93.

Waberski TD, Buchner H, Perkuhn M, Gobbele R, Wagner M, Kucker W, Silny J. N30 and the effect of explorative finger movements: a model of the contribution of the motor cortex to early somatosensory potentials. Clinical Neurophysiology, 1999; 110: 1589-600.

Wager TD, Rilling JK, Smith EE, Sokolik A, Casey KL, Davidson RJ, Kosslyn SM, Rose RM, Cohen JD. Placebo-induced changes in fMRI in the anticipation and experience of pain. Science, 2004; 303: 1162-67.

Wagner KJ, Willoch F, Kochs EF, Siessmeier T, Tolle TR, Schwaiger M, Bartenstein P. Dose-dependent regional cerebral blood flow changes during remifentanil infusion in humans: a positron emission tomography study. Anesthesiology, 2001; 94: 732-39.

Wang CC, Shyu BC. Differential projections from the mediodorsal and centrolateral thalamic nuclei to the frontal cortex in rats. Brain Research, 2004; 995: 226-35.

Whittingstall K, Stroink G, Gates L, Connolly JF, Finley A. Effects of dipole position, orientation and noise on the accuracy of EEG source localization. Biomedical Engineering Online., 2003; 2:14.

Willoch F, Tolle TR, Wester HJ, Munz F, Petzold A, Schwaiger M, Conrad B, Bartenstein P. Central pain after pontine infarction is associated with changes in opioid receptor binding: a PET study with 11C-diprenorphine. American Journal of Neuroradiology, 1999; 20: 686-90.

Wingate D, Hongo M, Kellow J, Lindberg G, Smout A. Disorders of gastrointestinal motility: Towards a new classification. Journal of Gastroenterology and Hepatology, 2002; 17: S1-S14.

Xie YF, Huo FQ, Tang JS. Cerebral cortex modulation of pain. Acta Pharmacologica Sinica, 2009; 30: 31-41.

Zhang YQ, Tang JS, Yuan B, Jia H. Inhibitory effects of electrically evoked activation of ventrolateral orbital cortex on the tail-flick reflex are mediated by periaqueductal gray in rats. Pain, 1997; 72: 127-35.